JOURNAL MOTION SIMULATION OF HYDRODYNAMIC JOURNAL BEARING CONSIDERING ELASTIC EFFECTS

A Thesis

Submitted in partial fulfillment of the requirements for the award of degree of

MASTER OF ENGINEERING
IN
CAD/CAM & ROBOTICS

By

HARSH VARDHAN SINGH
Roll No. 80681009

Under the guidance of

Dr. V. K. JADON
Associate Professor,
Deptt. of Mechanical Engg.
Thapar University, Patiala.

DEPARTMENT OF MECHANICAL ENGINEERING
THAPAR UNIVERSITY
PATIALA-147004, INDIA

JUNE, 2008

CERTIFICATE

This is to certify that the work which is being presented in this thesis entitled as **"JOURNAL MOTION SIMULATION OF HYDRODYNAMIC JOURNAL BEARING CONSIDERING ELASTIC EFFECTS"** submitted by Mr. Harsh Vardhan Singh, Registration No. 80681009, in partial fulfillment of the requirement for the award of degree of **MASTER OF ENGINEERING** in **CAD/CAM AND ROBOTICS** in the Mechanical Engineering Department, **THAPAR UNIVERSITY, PATIALA** is an authentic record of candidate's own work carried by him under the supervision and guidance of **Dr. V.K. Jadon,** Associate Professor, Mechanical Engineering Department, Thapar University, Patiala. The matter embodied in this thesis has not been submitted anywhere else for the award of any other degree.

(Dr. V.K. JADON)
Associate Professor,
Deptt. of Mechanical Engg.,
Thapar University,
Patiala, 147004.

Countersigned by:

10/3/08

(Dr. S.K. MOHAPATRA)
Professor and Head,
Deptt. of Mechanical Engg. ,
Thapar University,
Patiala, 147004.

(Dr. R.K.SHARMA)
Dean of Academic Affairs,
Thapar University,
Patiala, 147004.

The M.E. (Thesis) Viva Voce Examination of HARSH VARDHAN SINGH Roll No. 80681009, M.E. (CAD/CAM &Robotics), Thapar University, Patiala has been held on .....

Supervisor **External Examiner**

ACKNOWLEDGEMENT

I express my sincere gratitude to my guide, **Dr. V. K. Jadon, Associate Professor, Mechanical Engineering department**, **Thapar University**, **Patiala** for their valuable guidance, proper advice, painstaking and constant encouragement during the course of my work on this thesis.

I do not find enough words with which I can express my feeling of thanks to entire faculty and staff of **Mechanical Engineering department**, **Thapar Institute of Engineering & Technology**, **Patiala**, for their help, inspiration and moral support which went a long way in successful completion of my thesis.

HARSH VARDHAN SINGH

ABSTRACT

A journal bearing system, if disturbed from its equilibrium position, experiences change in the hydrodynamic forces acting on it. This disturbs the equilibrium of the journal and makes its centre to whirl around the static equilibrium position. The dynamic response of a journal bearing system under these conditions can be obtained using either linear or non-linear equation of motion of journal motion. The present work is aimed to determine the realistic dynamic response of hydrodynamic bearing.

In this work, the nonlinearized dynamic response of the journal bearing for both rigid and flexible bearing is studied by considering two cases of journal mass M_J with respect to critical mass $\overline{M_c^l}$ obtained from linear analysis .i.e. $\overline{M_J} = \overline{M_c^l}$ and $\overline{M_J} > \overline{M_c^l}$. The deviation in stability margins is established by comparing the results obtained from the linearized and nonlinearized stability analysis for elastohydrodynamic case. The coupled solution of Reynold's equation and elasticity equation is obtained using finite element method and the equation of motion is computed using fourth order Runga-Kutta method. The results obtained in the present work for nonlinear dynamic analysis of hydrodynamic bearing shows an increase in stability margin as compared to linear analysis for a case when isothermal conditions are assumed and bearing is considered flexible.

INDEX

CONTENTS **Page No.**

NOMENCLATURE

DIMENSIONAL PARAMETERS

c : Radial clearance (m)

D : Journal diameter (m)

e : Journal eccentricity (m)

F : Fluid-film reaction (N)

h : Fluid-film thickness (m)

L : Bearing Length (m)

N : Rotational speed (rpm)

O : Geometric center

p : Pressure ($N.m^{-2}$)

Q : Bearing flow ($m^3.sec^{-1}$)

R : Journal radius (m)

T : time (s)

u, v, w : Fluid velocity components in X, Y, Z direction ($m\ sec^{-1}$)

W : External load, N

x : Circumferential coordinate

X_J, Z_J : Journal center coordinate

X, Y, Z : Cartesian coordinate system

y : Axial coordinate

z : Coordinate along film thickness

μ : Dynamic viscosity (Pa.s)

μ_r : Reference viscosity (Pa. s)

ω_j : Journal rotational speed (s^{-1})

ω_{th} : Threshold speed (s^{-1})

NON-DIMENSIONAL PARAMETERS

$\bar{c} = \frac{c}{R_J}$

$\bar{C}_{ij} = C_{ij}\left(\frac{c^3}{\mu_r R_J^4}\right)$

$\bar{h}, \bar{h}_{min} = (h, h_{min})/c$

$\bar{p} = p/p_s$

$\bar{t} = t(c^2 p_s/\mu_r R_j^2)$

$\bar{F} = F\left(\frac{1}{p_s R_J^2}\right)$

$\bar{\varepsilon} = e/c$

$\bar{z} = \frac{z}{h}$

$\bar{r} = \frac{r}{R_J}$

$\bar{t} = t\left(\frac{c^2 p_s}{\mu_r R_J{}^2}\right)$

$\bar{u}, \bar{v} = (u, v)\left(\frac{\mu_r R_J}{c^2 p_s}\right)$

$\bar{W} = \frac{W}{p_s R_J^2}$

$\alpha, \beta = (x, y)/R_J$

$\lambda = L/D$

$\bar{\mu} = \mu/\mu_r$

Ω = Speed parameter

$$= \omega_J \left(\frac{\mu R_J^2}{c^2 p_s} \right)$$

$$\overline{m} = m \left(\frac{c p_s}{\mu_r \times R_J} \right)^{\frac{n-1}{2}} \left(\frac{R_J}{c p_s} \right)$$

MATRICES AND VECTORS

$[\overline{F}]$: Fluidity matrix

$[J]$: Jacobian matrix

$[N]$: Shape function matrix

$\{\overline{p}\}$: Nodal pressure vector

$\{\overline{Q}\}$: Nodal flow vector

$\{\overline{R}_H\}$: Column vector due to hydrodynamic terms

$[K]$: Stiffness matrix

$\{F_\Gamma\}$: System traction force vector

$\{\overline{\delta}\}$: Nodal displacement vector

LIST OF FIGURES

LIST OF TABLES

Chapter 1

INTRODUCTION

In today's world we are highly dependent upon the mechanical devices or machines for our daily works. The operation of these mechanical systems involves the relative motion of some machine elements. To protect the wear and tear of these relatively moving surfaces under various types of external loadings and to have better and smooth operation, we use bearings, which is the heart of every mechanical system/device or machine. Because of wide utility of bearing, continuous efforts are being carried out to improve the bearing mechanisms to have better relative motion of the parts by finding the suitably designed journal bearing with proper lubrication to get desired performance level.

Fluid-film bearings play a key role in the design of turbo machinery systems. They are important components of turbines, compressors, and pumps that are widely used in aircraft, naval ship as well as petrochemical, power and petroleum industries. Because of wide application of bearing, continuous efforts are being carried out to improve the bearing mechanisms to have the proper relative motion of the parts by finding the suitably designed bearing with proper lubrication to get desired performance level. Generally, the lubricants used to lubricate the journal bearings are mineral oils and additives are added to them to enhance their performance. The following sections give the details of types of journal bearings.

1.1 HYDRODYNAMIC JOURNAL BEARINGS

The journal bearings are mainly classified into two types namely, sliding journal bearing and roller element journal bearing. The sliding journal bearings are classified into three types namely: hydrodynamic, hydrostatic and hybrid journal bearing. In the

hydrodynamic journal bearing (figure 1.1), the journal drags liquid by viscous force in to the converging gap region between the two bearing surfaces. The converging gap region occurs on one half of the bearing between the maximum gap on one side and the minimum gap on the other. The result of the liquid being dragged in to a more confined region is to create a backpressure. This build up of pressure produce a bearing film force separating the two solid surfaces. The resultant of the bearing film forces, which act normally to the journal at each point around the bearing, will be equal and opposite of the externally applied force on the shaft. For given eccentricity of the journal with in the bearing, the pressure force giving rise to the hydrodynamic load is primarily dependent upon speed (n), viscosity (μ) and bearing projected area ($L \times D$).

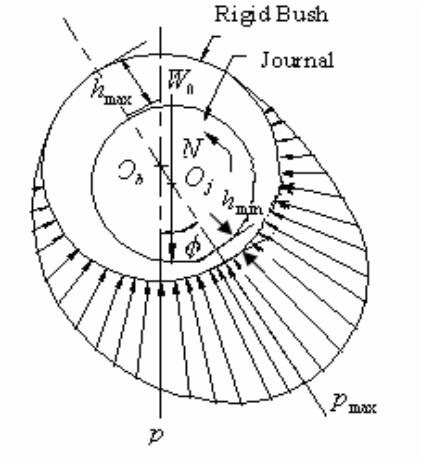

Figure 1.1

Radial Pressure Distributions on the Journal in Hydrodynamic Journal Bearing System

1.2 HYDROSTATIC BEARING

Hydrostatic bearings are of prime importance to the engineers as the machine parts supported on these bearings operate with incomparable smoothness. High load carrying capacity, increased minimum fluid film thickness, long life and increased support damping make them attractive of various precision applications such as turbo machinery, machine tool spindles and precision grinder spindles etc. The basic principle of hydrostatic bearing is to supply lubricant at high pressure to recesses in the bearing via

restrictors/flow control devices such as capillary, orifice, and constant flow valve, which lifts the journal against the load applied on it.

In the hydrostatic journal-bearing example shown in figure 1.2, liquid is introduced to four recesses through the separate entry ports. If the centre of the shaft were concentric with journal bearing, the pressure would be almost constant around the shaft. Restrictors are placed in the supply lines from the pump to each recess so that the magnitude of the recess pressure will normally be some value less than the pump supply pressure. The reason for this is to provide for varying recess pressure with the applied load on the bearing. The effect in the journal bearing may be demonstrated from the centre of the bearing. On the side where there is a reduction in the gap the flow from the recess is restricted and the recess pressure on this side rises. On the opposite side where the gap is increased the restriction to flow from the recess is reduced and hence pressure is reduced. It means the pressure on the opposite sides of the shaft is no longer in balance. Thus both side of the bearing contribute to the net bearing film force, and bearing film force must be equal and opposite of externally applied force. The main parameter, which governs the hydrostatic load, is the supply pressure and the projected bearing area.

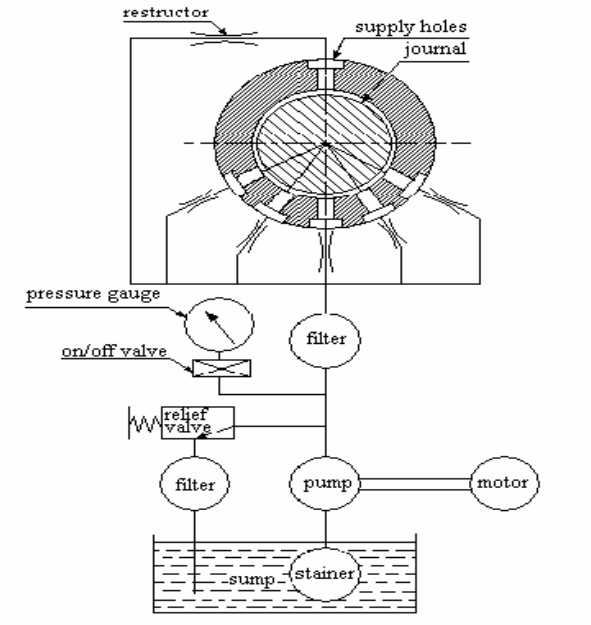

Figure 1.2

Hydrostatic Bearing System

1.3 HYBRID BEARING

The past conventional hydrostatic journal bearing were restricted to support heavy load at zero or low speed and also at low eccentricity required for precision machine. And also limitation of poor performance of hydrodynamic bearings at low speed compelled the designers to improve the performance of hydrostatic journal bearings and to develop alternative configurations in order to meet expanding industrial demands at different speeds. Therefore the hybrid journal bearings have been developed and used successfully in machines, which operates under high speed and heavy load conditions. A hybrid bearing combines the physical mechanisms of both hydrodynamic and hydrostatic bearings. The hybrid journal bearings can be classified into two types, namely: recessed bearing and non-recessed bearings. In the hybrid mode of operation the conventional hydrostatic/ hybrid bearings contribute very less towards hydrodynamic action on account of two reasons. First in the recess bearing, the recesses/ pockets occupy considerable portion of bearing land and thus the hydrodynamic action generated is not substantial when operating under high speed. Secondly the restrictors may allow the backward flow from a recess, which detracts from possible load support. Thus the recessed bearings when operating in hybrid mode at higher speed are not suitable for heavy loaded applications. A typical four pockets hydrostatic journal bearing is shown in figure 1.3 below.

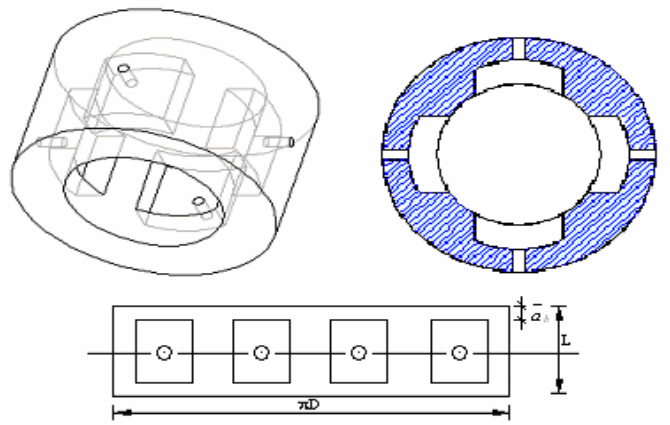

Figure 1.3

Symmetric Recessed Hole-Entry Journal Bearing Configuration with Four Square Recesses

Non-recessed bearings do not have any recess and they are preferred over recessed bearings because more hydrodynamic effect at high speeds as compared to recessed bearings can be generated because of higher bearing land area. In non-recessed bearings when operating under load, the developed fluid film pressure causes deformation of the bearing shell and consequently alters the fluid film profile. Non-recessed bearings used for hybrid operation to gain maximum advantage of both hydrostatic and hydrodynamic affects in a more efficient way. These types of bearings give better performance and these are easy to manufacture and have reduced manufacturing cost as compared to conventional recessed journal bearings.

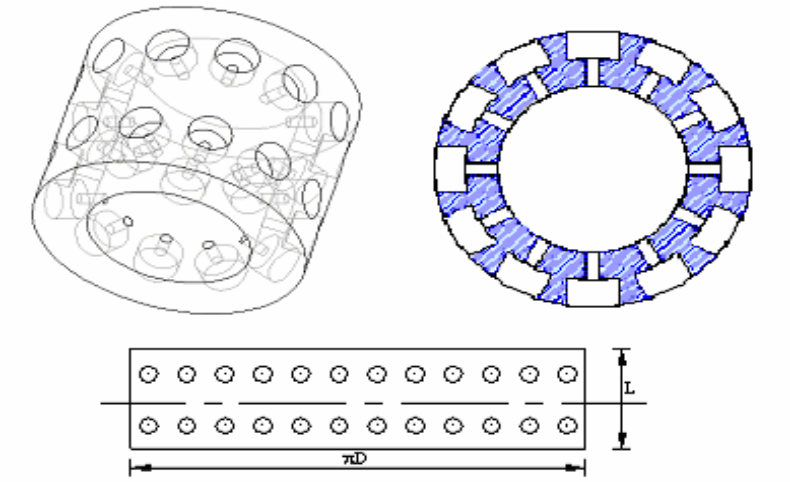

Figure 1.4

Symmetric Non-Recessed Hole-Entry Journal Bearing Configuration with 24 Holes

Hence these can be used as an alternative for recessed bearings. A typical non-recessed 24 holes symmetric hybrid journal bearing is shown in above figure 1.4. In non-recessed bearings, the different recess shapes can be used depending upon the requirements, which are, mainly circular, rectangular, elliptical, and triangular recesses.

In symmetric hybrid journal bearing holes are placed symmetrically and in case of asymmetric hybrid journal bearing the position of holes is not symmetric as shown in figure 1.5 and figure 1.6 respectively. The asymmetric configuration has an advantage of having higher load carrying capacity even at zero eccentricity as compared to symmetric configuration.

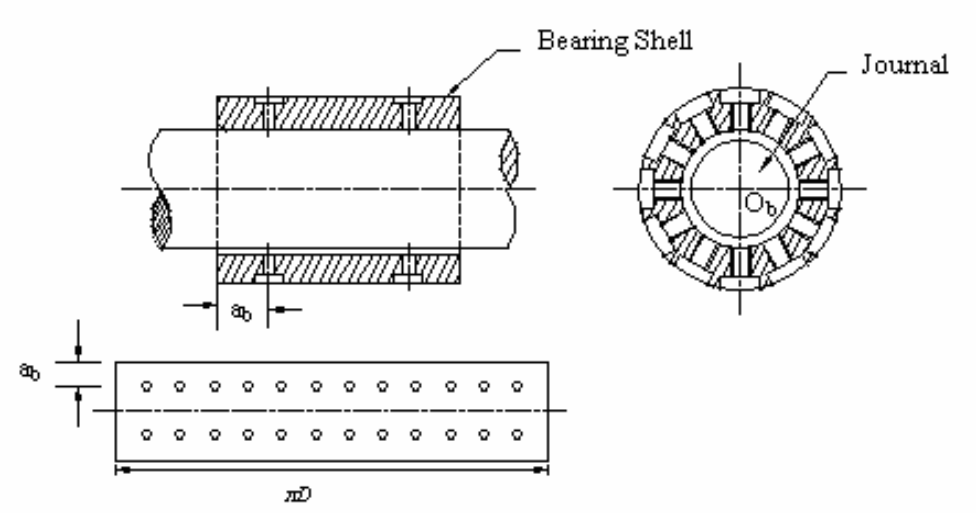

Figure 1.5

Symmetric Hole-Entry Journal Bearing

There can also be other hybrid journal bearing configurations having number of rows of holes and their positions.

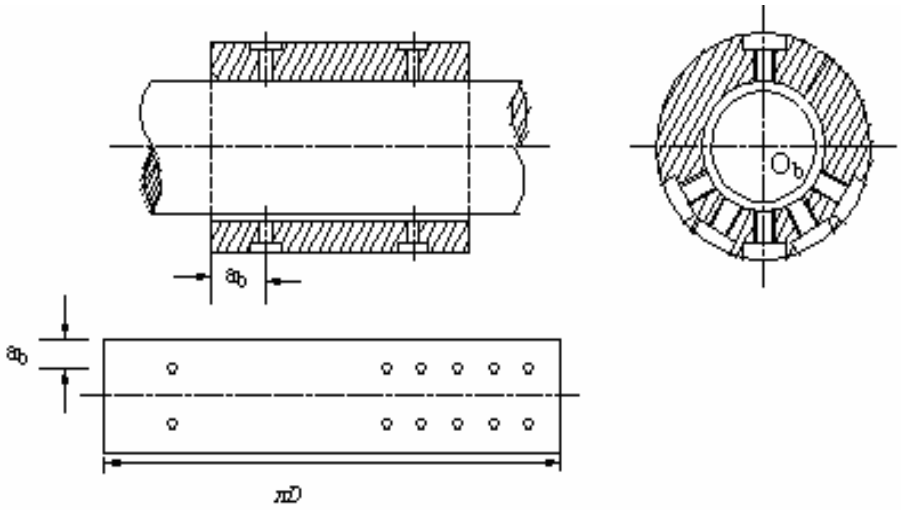

Figure 1.6

Asymmetric Hole-Entry Journal Bearing

1.4 PERFORMANCE CHARACTERISTICS

There are two types of performance characteristics of journal bearings.

1.4.1 STATIC PERFORMANCE CHARACTERISTICS

These characteristics include load carrying capacity, eccentricity ratio and attitude angle. Load carrying capacity is the capacity to carry the load by bearing. During operation of the journal bearing, the centre of the journal is offset from the centre of the bearing (bushing) by a distance e, called the eccentricity. The difference in radii, $c = R_2 - R_1$, is called the clearance and the ratio $\varepsilon = e/c$ is the eccentricity ratio. The angular distance between the load line and the position of minimum thickness is known as attitude angle.

1.4.2 DYNAMIC PERFORMANCE CHARACTERISTICS

Dynamic performance characteristics of a journal bearing system are expressed in terms of stiffness and damping coefficients. In fluid film bearings, the thin film separates the moving surfaces and supports the rotor load; it acts like a spring and provides the damping effect due to squeeze film effect. The stiffness and damping properties of the oil film significantly alter the critical speeds and out of balance response of rotor. Therefore, stiffness and damping coefficients plays a significant role in the analysis of journal bearing.

1.5 PRESENT WORK

The present work is related to determine realistic dynamic response of the hydrodynamic bearing considering elastic effects and assuming isoviscous lubricant. The journal centre motion is theoretically simulated to study the stability of journal bearing system. To simulate the journal centre motion, equations of motion are computed using fourth order Runga-Kutta method. Results are obtained for linearised and nonlinearised stability analysis to establish the deviation in stability margins. Nonlinearized dynamic response of the journal bearing system is studied by

considering two cases of journal mass with respect to critical mass ($\overline{M_c^l}$) obtained from linear analysis.

Case 1: Journal mass is equal to linear critical mass $\overline{M_J} = \overline{M_c^l}$.

Case 2:Journal mass is greater than linear critical mass $\overline{M_J} > \overline{M_c^l}$. Firstly, the linear and nonlinear trajectories are drawn by taking $\overline{M_J} = \overline{M_c^l}$ to observe the response of the journal obtained from the present formulation. The journal mass $\overline{M_J}$ is raised in increments so as limit cycle is obtained giving nonlinear critical mass $\overline{M_c^n}$. Thus, the nonlinear critical mass is the mass of the journal at which the nonlinear trajectory represents the limit cycle response. The difference between nonlinear critical mass and linear critical mass is studied for various loads and elastic deformation coefficient $C_d = 1$ and $C_d = 5$.

Chapter 2

LITERATURE REVIEW

In order to theoretically simulate the journal motion, the related literature is studied. The following section details the literature available and relevant to the present study.

M.O.A. Mokhtar et al [1] investigated experimentally, the behavior of plain hydrodynamic journal bearings during starting and stopping. They observed and analyzed the effects of load, speed, and bearing clearance on the journal movements. They concluded that during the starting a rapid buildup of hydrodynamic forces occurred in all cases. A hydrodynamic film was formed in a very short time, after which the shaft moved in a spiral shaped whirling locus to the steady state operating position. Prior to separation of the shaft and bearing surfaces, the contact was mainly a sliding situation with little or no initial rolling. At stopping, the shaft followed a typical hydrodynamic locus until rotation ceased and then a squeeze film trajectory to the final resting position.

Shangxian Xu [2] set up a new bearing test rig for static and dynamic tests of oil-film journal bearings. Micro pressure and displacement transducers contained in shaft measure the distribution of oil film pressure and thickness, and two electromagnetic exciters are located under and behind the test bearing to excite the test bearing in order to obtain its eight dynamic stiffness and damping coefficients. A misalignment jig was re-employed to align or misalign the test bearing with respect to the axis of the shaft. Valuable performance results were obtained for a recessed hydrostatic bearing, a slot-entry hybrid bearing, and a hole-entry hybrid bearing. The results of the test bearing are basically in agreement with the theoretical analysis values at low eccentricity, but

deviation at high eccentricity ratio might be due to the simplicity of the mathematical model in theoretical analysis and a number of factors which caused the test deviation.

Ronald d. Flack et al [3] developed a bearing test rig to characterize the static and dynamic properties of hydrodynamic journal bearings. Static measurement capabilities include operating eccentricity, pressure and thermal boundary conditions, and continuous circumferential pressure and film thickness profiles at multiple axial planes. Dynamic stiffness and damping coefficient measurements are achieved using steady state harmonic excitations generated by a two-axis shaker system. All essential data for a complete understanding of one particular bearing can be collected simultaneously. To ensure high quality results, the rig was designed to minimize the influence of measurement uncertainties on the derived dynamic coefficients. They described complete details. Consistent results were attributed to the use of a comprehensive uncertainty analysis in the design process and to a good match between the actual implementation of the test and the assumed linear bearing model.

Vijay kumar et al [4] studied the transient response of capillary compensated hybrid journal bearing system during starting and stopping operation. They theoretically computed the journal trajectories during acceleration, deceleration, and with uniform motion of journal. The results of the journal bearing system with non-recessed hole entry is computed by solving the momentum and continuity equations governing the laminar flow of an incompressible Newtonian lubricant in the clearance space of finite journal bearings. They solved the coupled equations; Reynolds equation and the equation of the restrictor employed in the flow field. The effect of cavitation is also considered.

An Sung Lee et al [5] presented a finite element transient response analysis method of a rotor-bearing system to base shock excitations. The study involves applying the generalized finite element modeling method of a rotor-bearing system considering a base-transferred shock force along with the State-Space Newmark method of a direct time integration scheme based on the average velocity concept. They performed experiments to a test rig of a mock-up rotor-bearing system with a series of half-sine shock waves imposed by an electromagnetic shaker and compared the experimental results with theoretical results. The analytical results agree quite well with the

experimental data. The results show that the transient responses of the rotor are sensitive to the duration times of the shocks.

Guangyan Shen et al [6] presented a model to calculate the fluid film forces of a fluid-film bearing with the Reynolds boundary condition by using the free boundary theory and the variational method. This paper presents a fast and accurate model to calculate the fluid-film forces of a fluid film bearing. Since the model is semi-analytical, it can be applied to many kinds of bearings, such as cylindrical bearings, partial arc bearings and multilobe bearings. It is not only applicable for short bearings and long bearings, but for finite length bearings as well. Both the balanced and unbalanced rotors are taken into consideration. The model is applied to the nonlinear dynamical behavior analysis of a rigid rotor in the elliptical bearing support. The balanced rotor undergoes a supercritical Hopf bifurcation as the rotor spin speed increases. The investigation of the unbalanced rotor indicates that the motion can be a synchronous motion, sub harmonic motion, quasi-period motion, or chaotic motion at different rotor spin speeds.

M. Malik et al [7] theoretically investigated the transient response of plane hydrodynamic journal bearing system during acceleration and deceleration periods. The nature of theoretically predicted journal response during starting and stopping is found lo be similar to the experimental behaviour reported by other authors. The motion of an accelerating or decelerating journal shows concurrence with the linearized stabilily charts. An interesting finding is that, beginning from an equilibrium state, a journal can be accelerated only to a limiting value so that it may return to its original state on being decelerated from the accelerated speed.

Cheng-chi wang and cha'o-ku`ang chen [8] presented a time-dependent mathematical model for gas journal bearings. They used system state trajectory, power spectra, and bifurcation diagrams to analyze the dynamic behavior of the rotor center in the horizontal and vertical directions under different operating conditions. The analysis shows how the existence of a complex dynamic behavior comprising periodic and subharmonic response of the rotor center. The paper shows how the dynamic behavior of this type of system varies with changes in rotor mass and rotational velocity.

Jiun-shen wang and cheng-chi wang [9] presented a numerical analysis of a rigid rotor supported by relative short aerodynamic journal bearings for nonlinear

dynamic behaviors and bifurcation. The analysis shows how the existence of a complex dynamic behavior comprises periodic and subharmonic response of the rotor center. This paper shows how the dynamic behavior of this type of system varies with changes in bearing number and squeeze number.

G. Grau et al [10] presented a numerical analysis of the static and dynamic performance of a compliant journal gas bearing. The common approach found in foil bearing literature consists in calculating the carrying capacity for a given shaft position. In this study the external load is fixed (magnitude and direction) and the related shaft position is investigated. Nevertheless, a rigid profile, able to support high imposed loads, is no longer valid if one considers that the bearing becomes compliant. An original calculation method of the initial profile considering rigid surfaces is proposed to overcome this problem. The prediction of nonlinear dynamic behavior, i.e., stability and response to external excitation, is investigated. Finally, a viscous damping model is introduced into the dynamic model in order to obtain the amount of structural damping necessary to increase the stability of the compliant journal gas bearing.

S. K. Kakoty and b. C. Majumdar [11] studied the effect of fluid inertia on whirl instability of flexibly supported finite journal bearings by carrying out a non-linear time transient analysis. He reported that fluid inertia in stability analysis can not be ignored in the case of flexibly supported journal bearings. Consideration of fluid inertia in the analysis of a flexibly supported bearing would give accurate prediction.

Malik et al [12] presented "an assessment of the stability chart of linearized gas-lubricated plane journal bearing system". In this paper they assessed the stability chart of a linearized self-acting gas journal bearing by tracing the response of a journal accelerated from an equilibrium state. They obtained the response by the simultaneous time marching solution of the time-transient Reynolds equation and the equations of motion of the journal.

Rao et al [13] presented "a methodology for dynamic coefficients and nonlinear response of multi-lobe journal bearings". An easy to implement finite perturbation method is used to evaluate stiffness and damping coefficients. In order to obtain the fluid film forces, the oil film pressure generated in the bearing is solved using a semi analytical pressure model. The results are provided in graphical form and compared with existing

numerical techniques. The journal center trajectories obtained are compared with numerical results and the effect of stability on rotor beating system is studied for both balanced and unbalanced rotor. It is concluded that the approximate bearing solutions which are predominantly applied lo cylindrical bearing configuration, can also be successfully implemented for noncircular profiles.

Sanxing Zhao et al [14] established the motion equations for symmetrical single-disk flexible rotor-bearing system, and calculated non-linear oil-film forces of finite journal bearings. They considered the rotor's stiffness and damping also. The motions of journal and disk have been simulated with fourth-rank Runge-kutta method.

S.C. Jain et al [15] determined the journal motion trajectories using nonlinear equations of motion including the deformation of the bearing shell. They draw trajectories and time displacement plots to investigate the effect of bearing deformation on the dynamic performance of the journal bearing system. The study reveals the important changes in the dynamic response of the journal bearing system if inherent bearing flexibility is accounted in the analysis. Bearing deformation appreciably affects the dynamic response of the journal bearing system. The complaint bearing provides more damping to the journal bearing system. They concluded that the bearing deformation may improve the stability zone of the journal bearing system if suitably designed.

Vijay Kumar et al [16] investigated the restrictor design parameter of a capillary compensated hole–entry hybrid journal bearing system for optimum stiffness and dynamic coefficients of the bearing. In the study bearing flexibility and variation of viscosity due to temperature rise of the lubrication was considered. The results of the study indicate that change in viscosity of lubricant and bearing flexibility affects the bearing design parameter, so the stability of rigid rotor also gets affected.

A. K. Tieu et al [17] investigated the relationship between the stability contour determined from the nonlinear simulation and that from the linear theory. They obtained nonlinear bearing forces directly from the bearing pressure distribution which is solved from the Reynolds equation at each journal position. They simulated typical whirling trajectories under impact excitation, position perturbation and synchronous unbalance excitations and presented them to explain the stable, critical and unstable phenomena.

D.V. Singh et al [18] solved the fluid film lubrication equation for hydrostatic journal bearing by finite element method for determining its steady state performance and stiffness and damping coefficients. They determined motion trajectories of the journal centre by discritizing time using Runge-Kutta method, for a small arbitrary disturbance.

S.K. Bhargava and M. Malik [19] presented an assessment of the stability margin of plane hydrodynamic journal bearing system mounted on flexible damped pedestals. They expressed stability margin in term of critical speed (or critical mass) of journal. The assessment investigations were carried out by delineating the motion of an accelerating or decelerating journal.

Hiromu Hashimoto at el [20] theoretically examined the relations between journal centre motion trajectories and the variation in corresponding pressure distribution in rotor bearing system supported by two-lobe hydrodynamic journal bearings based on a nonlinear analysis. In order to obtain the values for the oil film forces used in the equations of motion for rotor bearing systems, they solved the Reynolds equation using the semi analytical finite element method at each time step. They concluded that the stability journal centre motion trajectory is strongly related to the variation in pressure distribution.

M. Malik and S. K. Bhargava [21] established a theoretical analysis for the transient response of a short journal bearing system with a flexible rotor and damped flexible pedestals. The transient response analysis was used to assess the linearized system stability chart and determine the journal motion during stopping and starting periods. The paper also includes some detailed results for the limiting speeds of short bearings.

T. V. V. L. N. RAO et al [22] developed analytical expressions for accurate evaluation of dynamic coefficients and prediction of post whirl orbits (transient journal center motion above instability critical speed) by computation of nonlinear journal trajectory for a cylindrical journal bearing.

L U'Yan-jun et al [23] investigated the nonlinear dynamic behaviors of a rotor dynamical system with finite hydrodynamic bearing supports. They presented a method consisting of a predictor-corrector mechanism and Newton-Raphson method to calculate equilibrium position and critical speed corresponding to Hopf bifurcation point of the

bearing-rotor system. The local stability and bifurcation behaviors of periodic motions are analyzed by the Flequet theory.

V. Meruane et al [24] obtained journal response from a computational fluid dynamic (CFD) model of a plain journal bearing on high dynamic loading conditions. The model considers fluid–structure interaction between the fluid flow and the journal. The case in study considers a laboratory test rig. Results indicate that nonlinear coefficients have an important effect on stiffness and damping. It was found a change on nonlinear behavior occurred when the Oil Whirl phenomenon starts, which it is not seen in classical linear models.

D. W. Parkins [25] described a novel experimental procedure for measuring the four velocity or damping coefficients of an Oil Film Journal Bearing from imposed dynamic orbits. All four damping coefficients are derived from one imposed journal center dynamic orbit and, therefore, may be regarded as being obtained at the same time. The method requires the production of a "figure of eight" shaped orbit and utilizes the "cross-over" point therein.

F. K. Choy et al [26] presented a simulation of a hydrodynamic journal bearing under various loading conditions. The procedure for the fluid film pressure solution involves an iterative scheme that solves the Reynolds equation. The pressure curve was integrated to calculate bearing supporting forces. Newton-Raphson iteration method was used to locate the journal equilibrium position from which both linear and nonlinear bearing stiffness are evaluated by means of the small perturbation technique. They analyzed effects of load on the linear/nonlinear plain journal bearing characteristics.

B. S. Prabhu et al [27] studied various design criteria for hydrodynamic bearings. They presented Results for unbalance response, dissipation coefficient, maximum transmitted force, stress amplitudes and fatigue life in the case of an industrial electric molar rotor supported on partial journal bearings using the transfer matrix method.

Ram Turaga et al [28] performed a non-linear transient stability analysis to study the sub-synchronous whirl stability of a rigid rotor supported on two symmetric hydrodynamic bearings with rough surfaces subjected to a unidirectional constant load. they solved a Reynolds type equation for finite hydrodynamic bearings, with different

models of rough surfaces using the stochastic finite element method. The trajectories of the journal center have been obtained by solving the equations of motion of the journal center by the fourth-order Runge-Kutta method. Results show an increase in the stability with transverse roughness and a decrease in the stability with isotropic roughness. A small improvement in stability is obtained with longitudinal roughness.

F.K. Choy et al [29] examined the nonlinear characteristics of hydrodynamic journal bearing. Results based on bearing stiffness characteristics, steady and transient vibration orbits, and frequency response functions obtained from both linear and nonlinear bearing simulations are compared with each other. Conclusions are drawn from the results obtained from a prototypical bearing configuration used as an example in this analysis.

Renato Brancati et al [30] determined synchronous orbits and orbits with a 5 component described by the journal with reference to a rigid symmetrical unbalanced rotor on lubricated journal bearings. The method also makes it possible to evaluate the stability of the above solutions and thus of the journal orbital motion.

Vijay Kumar et al [31] studied the stability margin of a constant flow valve compensated hole-entry hybrid journal bearing system considering bearing flexibility and variation of viscosity due to temperature rise of the lubricant. The results presented in the study indicate that the bearing flexibility and temperature rise of the lubricant fluid-film affects the performance of the hole-entry hybrid journal bearing system quite significantly and proper selection of restrictor design parameter is quite useful in maintaining the fluid film thickness and threshold speed of the journal.

The survey presented above indicates that investigations on dynamic response of journal bearing attracted a large number of researchers during last decades, but the studies remained confined mainly to linearized dynamic response. Researchers did not concentrate more on nonlinearized dynamic response. The nonlinearized dynamic response presents more realistic picture of journal bearing system. In study of linearized dynamic response, it is assumed that the hydrodynamic forces in the journal can be regarded as linear functions of the displacements and the velocity vectors. The equation of disturbed motion of the journal is written by equating the inertia force to the stiffness and the damping forces. The linearized dynamic response is reasonably accurate if the

journal centre perturbations are very much in the close neighbourhood of the static equilibrium position. The stiffness and damping coefficients (as used in linear model) for large disturbance is no longer remain constant and their values are altered for every new position of the journal centre. Therefore it is more realistic to use nonlinearized model to study dynamic response than linearized model.

S.C. Jain et al [15] drew trajectories and time displacement plots to investigate the effect of bearing deformation on the dynamic performance of the journal bearing system. They concluded that bearing deformation appreciably affects the dynamic response of the journal bearing system. The study, interestingly finds the improved stability margin for the journal system when elastic nature of the bearing is considered. This result also matches with present work, the stability margin increases when elastic nature of bearing is considered.

Chapter 3

ANALYSIS

This Chapter describes the generalized formulation of elastohydrodynamic (EHD) problem concerning hydrodynamic journal bearings. Mathematically, EHD studies involve simultaneous solutions of Reynold's and elasticity equations. The generalized Reynold's equation governing lubricant flow field is used to determine the pressure distribution in the clearance space between journal and bearing. The fluid-film pressure causes deformation in the bearing bush. These deformations are computed by using 3D elasticity equation.

For a journal bearing system, the journal rotating with uniform speed at equilibrium position, is termed as the steady state at which the static performance characteristics ($\overline{p}_{\max}$, $\overline{h}_{\min}$, ϕ etc.) are obtained. The dynamic performance characteristics include fluid-film stiffness and damping coefficients and the computation of these coefficients requires pressure derivatives with respect to displacement and velocity components of the journal. The expressions for the bearing stability parameters i.e. critical mass and threshold speed are also derived in this chapter using the linearized equations of the journal center and Routh's criteria.

The journal shifts from its equilibrium position due to external disturbances. This causes dynamic force on the journal in addition to those acting at the steady-state condition. These forces make the journal to whirl around its static equilibrium position and are functions of the journal center displacement and velocity components. The study of the dynamic response of the disturbed motion of journal is carried out using linear equation written in terms of linearized stiffness and damping coefficients and nonlinear equation of motion as well. In the present work both the method are used for the study of

dynamic response and the relevant equations of motion are described in this chapter.

In the following, the representative mathematical models for the lubricant flow field and the bearing displacement field with boundary conditions are presented. The mathematical models for journal centre motion trajectories are also obtained.

3.1 FLOW FIELD EQUATION

The theory of hydrodynamic lubrication is based on differential equation derived by Obsorne Reynold. Reynold's equation is based on the following assumptions:

1. Body forces are neglected, which means that there is no outside field of force acting on the lubricant such as gravitational or magnetic forces, etc.
2. The pressure is considered to be constant through the thickness of the film. As the oil film very thin, the pressure cannot vary significantly across it.
3. The curvatures of the bearing surfaces are considered to be large compared with the oil film thickness. The surface velocities need not therefore be taken as varying in direction.
4. There is no slip at the boundaries, which means that the velocity of the surface is same as the velocity of the final, adjacent, layer of lubricant.
5. The lubricant is Newtonian.
6. The flow is laminar.
7. The fluid inertia can be neglected.
8. The viscosity of lubricant is constant.

An element having dimensions dx, dy and dz is considered in this analysis, and is shown in figs 3.1 and 3.2. X is the axis in the direction of motion, Y is the axis parallel to the axis of journal and Z is the axis in the radial plane. u, v and w are the velocities in X,Y and Z directions respectively. τ_x and τ_y are shear stresses along X and Z directions, while p is the fluid film pressure.

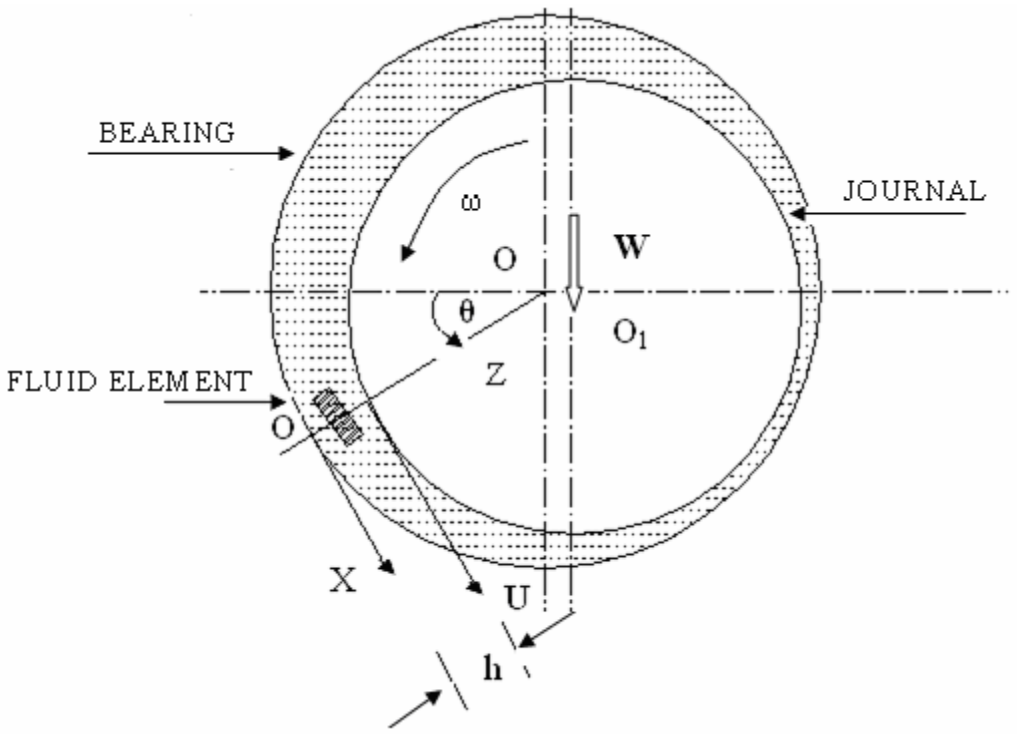

Fig.3.1

Location of Fluid Element in X-Y Plane

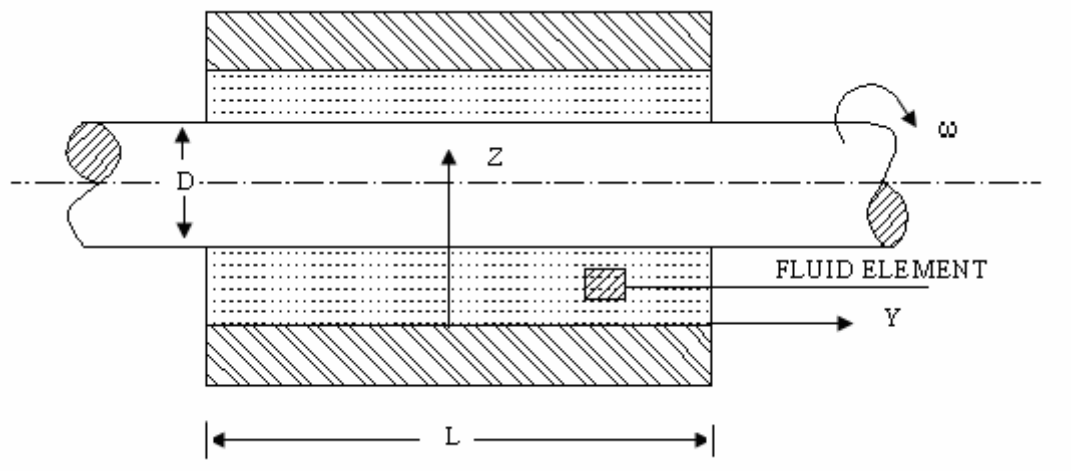

Fig3.2

Location of Fluid Element in Y-Z Plane

The forces acting on the element in the X direction are shown in figure 3.3.

Considering equilibrium of forces,

$$\left(\frac{\partial \tau x}{\partial z} dz\right)(dxdy) = \left(\frac{\partial p}{\partial x} dx\right)(dydz) \qquad (3.1)$$

Since (dx x dy x dz) indicates the volume of the element, therefore

(dx x dy x dz) ≠ 0

The equation (3.1) is written as

$$\frac{\partial \tau x}{\partial z} = \frac{\partial p}{\partial x} \qquad (3.2)$$

According to Newton's law of viscosity

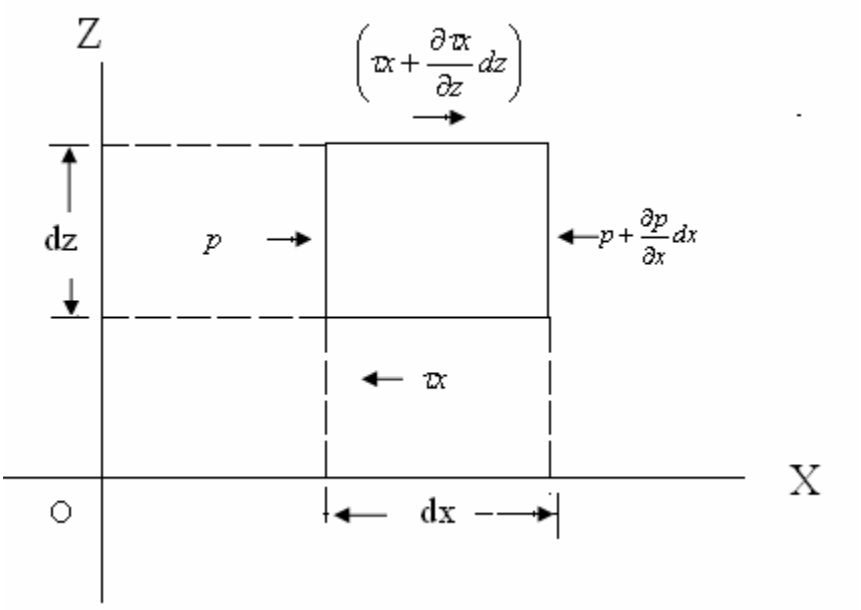

Fig.3.3

Equilibrium of Forces in X Direction

$$\tau x = \mu \frac{\partial u}{\partial z} \qquad (3.3)$$

From equation (3.2) & (3.3)

$$\frac{\partial^2 u}{\partial z^2} = \frac{1}{\mu} \frac{\partial p}{\partial x}$$

Integrating twice

$$u = \frac{1}{\mu}\frac{\partial p}{\partial x}\frac{z^2}{2} + C_1 z + C_2 \qquad (3.4)$$

The constants C_1 and C_2 of integration are evaluated from boundary conditions,

u = 0 when z=0

u = U when z=h

Substituting these boundary conditions in equation (3.4)

$C_2 = 0$

$$C_1 = \frac{U}{h} - \frac{1}{\mu}\frac{\partial p}{\partial x}\frac{h}{2} \qquad (3.5)$$

Substituting these values in equation (3.4)

$$u = \frac{Uz}{h} + \frac{1}{2\mu}\frac{\partial p}{\partial x}\left(z^2 - hz\right) \qquad (3.6)$$

The forces acting on the element in the Y direction are shown in figure 3.4 . Considering equilibrium of forces,

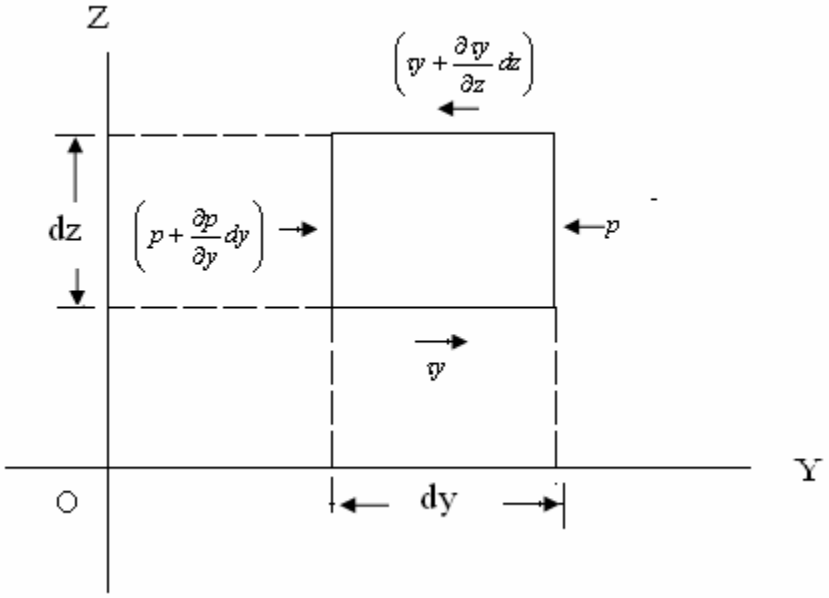

Fig.3.4

Equilibrium of Forces in Y Direction

$$\left(\frac{\partial \tau y}{\partial z} dz\right)(dxdy) = \left(\frac{\partial p}{\partial y} dy\right)(dxdz) \qquad (3.7)$$

Since (dx x dy x dz) ≠ 0

The equation (3.7) is written as

$$\frac{\partial \tau y}{\partial z} = \frac{\partial p}{\partial y} \qquad (3.8)$$

According to Newton's law of viscosity

$$\tau y = \mu \frac{\partial y}{\partial z} \qquad (3.9)$$

From equation (3.8) & (3.9)

$$\frac{\partial^2 y}{\partial z^2} = \frac{1}{\mu}\frac{\partial p}{\partial y}$$

Integrating twice

$$y = \frac{1}{\mu}\frac{\partial p}{\partial y}\frac{y^2}{2} + C_3 y + C_4 \qquad (3.10)$$

The constants C_3 and C_4 of integration are evaluated from boundary conditions,

v = 0 when z=0

v = 0 when z=h

Substituting these boundary conditions in equation (3.10)

$C_4 = 0$

$$C_3 = -\frac{1}{\mu}\frac{\partial p}{\partial y}\frac{h}{2}$$

Substituting these values in equation (3.10)

$$v = \frac{1}{2\mu}\frac{\partial p}{\partial y}\left(z^2 - hz\right) \qquad (3.11)$$

Now the rate of lubricant flow in the X direction is the integral $\int_0^h u dz$, let this denoted by q_x and similarly $q_y = \int_0^h v dz$. Both q_x and q_y are the rates of flow per unit width. Thus from equation (3.6)

$$q_x = \int_0^h u\,dz = \frac{Uz^2}{2h}\Bigg|_0^h + \frac{1}{2\mu}\frac{\partial p}{\partial x}\left(\frac{z^3}{3} - \frac{hz^2}{2}\right)\Bigg|_0^h$$

$$q_x = \frac{Uh}{2} - \frac{h^3}{12\mu}\frac{\partial p}{\partial x} \qquad (3.12)$$

And exactly in the same way

$$q_y = -\frac{h^3}{12\mu}\frac{\partial p}{\partial y} \qquad (3.13)$$

Now if the two surfaces pulsate with velocities w_h for the upper surface and w_o for the lower one, the simple continuity equation will need to be

$$\frac{\partial q_x}{\partial x} + \frac{\partial q_y}{\partial y} + \frac{\partial q_z}{\partial z} = 0 \qquad (3.14)$$

Now the layer of fluid immediately touching each of the surfaces will move with velocity w_h and w_o. If unit surface area is considered this corresponds to a swept volume of wh and wo per unit time, i.e. a rate of flow of w_h and w_o. Hence the difference of flow over the two surfaces $\frac{\partial q_z}{\partial z} = \left(w_h - w_o\right)$. Then now in continuity equation

$$\frac{\partial}{\partial x}\left(\frac{Uh}{2} - \frac{h^3}{12\mu}\frac{\partial p}{\partial x}\right) + \frac{\partial q_y}{\partial y}\left(-\frac{h^3}{12\mu}\frac{\partial p}{\partial y}\right) + \left(w_h - w_o\right) = 0$$

or

$$\frac{\partial}{\partial x}\left(h^3\frac{\partial p}{\partial x}\right) + \frac{\partial}{\partial y}\left(h^3\frac{\partial p}{\partial x}\right) = 6\mu\left\{U\frac{dh}{dx} + 2\left(w_h - w_o\right)\right\} \qquad (3.15)$$

This is the Reynold's equation in three dimensions.

In case of journal bearing the bearing is fixed, therefore wo=0.

Now the term $\left(w_h - w_o \right)$ can be written as $\frac{dh}{\partial t}$, where h is the film thickness and t is time. Now the Reynold's equation becomes

$$\frac{\partial}{\partial x}\left(h^3 \frac{\partial p}{\partial x} \right) + \frac{\partial}{\partial y}\left(h^3 \frac{\partial p}{\partial y} \right) = 6\mu \left\{ U \frac{dh}{dx} + 2\frac{dh}{\partial t} \right\} \qquad (3.16)$$

The above equation in non-dimensional form may be written as

$$\frac{\partial}{\partial \alpha}\left(\bar{h}^3 \frac{\partial \bar{p}}{\partial \alpha} \right) + \frac{\partial}{\partial \beta}\left(\bar{h}^3 \frac{\partial \bar{p}}{\partial \beta} \right) = \frac{\partial \bar{h}}{\partial \alpha} + 2\frac{\partial \bar{h}}{\partial \bar{t}} \qquad (3.17)$$

Where

$$h = c\bar{h} \qquad y = L\bar{y} \qquad p = 6\omega\mu \frac{R^2}{c^2} \bar{p}$$

$$\bar{t} = \omega t$$

3.1.1 BOUNDARY CONDITIONS

The pressure stars at the start of the bearing arc, except in the case of the 360^0 bearing when it starts at the position of maximum film thickness (θ = 0). In practice bearings are usually split at $\pm 90^0$ to the load line, to make 180^0 bearing, and so this is the most important case. Even in the 360^0 bearings the pressure usually starts late, at about 90^0 to the load line.

The pressure is taken as ending where the gradient is zero, at some point θ > π, i.e. $p = \frac{dp}{d\theta} = 0$ at θ = π+α.

3.1.2 FLUID-FILM THICKNESS

For a rigid journal bearing system, operating under static conditions, the fluid film thickness expression is given as [20]:

$$\bar{h} = 1 - \bar{X}_J \cos\alpha - \bar{Z}_J \sin\alpha \qquad (3.18)$$

Where, $\bar{h}$ is the fluid-film thickness, when the journal center is in static equilibrium position.

3.1.3 FINITE ELEMENT FORMULATION

Lubricant flow field has been discretized using four-noded quadrilateral isoparametric elements. The pressure variation is assumed to vary linearly over an element. The Reynold's equation in non-dimensional form is

$$\frac{\partial}{\partial\alpha}\left(\bar{h}^3\frac{\partial\bar{p}}{\partial\alpha}\right)+\frac{\partial}{\partial\beta}\left(\bar{h}^3\frac{\partial\bar{p}}{\partial\beta}\right)=\frac{\partial\bar{h}}{\partial\alpha}+2\frac{\partial\bar{h}}{\partial\bar{t}} \qquad (3.19)$$

$\frac{\partial\bar{h}}{\partial\bar{t}}$ is given by

$$\frac{\partial\bar{h}}{\partial\bar{t}}=-\overline{\dot{X}_j}\cos\alpha-\overline{\dot{Z}_j}\sin\alpha$$

Now Reynold's equation in non-dimensional form is

$$\frac{\partial}{\partial\alpha}\left(\bar{h}^3\frac{\partial\bar{p}}{\partial\alpha}\right)+\frac{\partial}{\partial\beta}\left(\bar{h}^3\frac{\partial\bar{p}}{\partial\beta}\right)=\frac{\partial\bar{h}}{\partial\alpha}-2\overline{\dot{X}_j}\cos\alpha-2\overline{\dot{Z}_j}\sin\alpha$$

Using Orthogonality condition of Galerkin's method, we have:

$$\sum_{e=1}^{n_e}\left[\iint_{\bar{A}^e}\left\{\frac{\partial}{\partial\alpha}\left(\bar{h}^3\frac{\partial\bar{p}}{\partial\alpha}\right)+\frac{\partial}{\partial\beta}\left(\bar{h}^3\frac{\partial\bar{p}}{\partial\beta}\right)-\frac{\partial\bar{h}}{\partial\alpha}+2\overline{\dot{X}_j}\cos\alpha+2\overline{\dot{Z}_j}\cos\alpha\right\}N_i\,d\alpha d\beta\right]=0 \qquad (3.20)$$

Where, n_e = Total no. of elements and i = 1, 2, 3 …… n (no. of nodes per element)

Part wise integration of second order terms of equation 3.20, we get

$$\iint_{\bar{A}^e}\frac{\partial}{\partial\alpha}\left(\bar{h}^3\frac{\partial\bar{p}}{\partial\alpha}\right)N_i\,d\alpha d\beta=\int\bar{h}^3\frac{\partial\bar{p}}{\partial\alpha}N_i\,d\beta-\iint_{\bar{A}^e}\bar{h}^3\frac{\partial\bar{p}}{\partial\alpha}\frac{\partial N_i}{\partial\alpha}\,d\alpha d\beta$$

Or,
$$\iint_{\bar{A}^e}\frac{\partial}{\partial\alpha}\left(\bar{h}^3\frac{\partial\bar{p}}{\partial\alpha}\right)N_i\,d\alpha d\beta=\int_{\bar{\Gamma}^e}\bar{h}^3\frac{\partial\bar{p}}{\partial\alpha}l_1N_i\,d\bar{\Gamma}^e-\iint_{\bar{A}^e}\bar{h}^3\frac{\partial\bar{p}}{\partial\alpha}\frac{\partial N_i}{\partial\alpha}\,d\alpha d\beta$$

Similarly,

$$\iint_{\bar{A}^e}\frac{\partial}{\partial\beta}\left(\bar{h}^3\frac{\partial\bar{p}}{\partial\beta}\right)N_i\,d\alpha d\beta=\int\bar{h}^3\frac{\partial\bar{p}}{\partial\beta}N_i\,d\alpha-\iint_{\bar{A}^e}\bar{h}^3\frac{\partial\bar{p}}{\partial\beta}\frac{\partial N_i}{\partial\beta}\,d\alpha d\beta$$

Or, $$\iint_{\bar{A}^e} \frac{\partial}{\partial \beta}\left(\bar{h}^3 \frac{\partial \bar{p}}{\partial \beta}\right) N_i d\alpha d\beta = \int_{\bar{\Gamma}^e} \bar{h}^3 \frac{\partial \bar{p}}{\partial \beta} l_2 N_i d\bar{\Gamma}^e - \iint_{\bar{A}^e} \bar{h}^3 \frac{\partial \bar{p}}{\partial \beta} \frac{\partial N_i}{\partial \beta} d\alpha d\beta$$

Also

$$\iint_{\bar{A}^e} \frac{\partial \bar{h}}{\partial \alpha} N_i d\alpha d\beta = \int_{\beta} \bar{h} N_i d\beta - \iint_{\bar{A}^e} \bar{h} \frac{\partial N_i}{\partial \alpha} d\alpha d\beta$$

Or, $$\iint_{\bar{A}^e} \frac{\partial \bar{h}}{\partial \alpha} N_i d\alpha d\beta = \int_{\Gamma^e} \bar{h} N_i l_1 d\Gamma^e - \iint_{\bar{A}^e} \bar{h} \frac{\partial N_i}{\partial \alpha} d\alpha d\beta$$

Substituting these values in equation 3.20, the equation becomes as below:

$$\sum_{e=1}^{n_e} \left[\int_{\bar{\Gamma}^e} \left(\bar{h}^3 \frac{\partial \bar{p}}{\partial \alpha} l_1 + \bar{h}^3 \frac{\partial \bar{p}}{\partial \beta} l_2 \right) N_i d\bar{\Gamma}^e - \iint_{\bar{A}^e} \left\{ \bar{h}^3 \left(\frac{\partial \bar{p}}{\partial \alpha} \frac{\partial N_i}{\partial \alpha} + \frac{\partial \bar{p}}{\partial \beta} \frac{\partial N_i}{\partial \beta} \right) \right\} d\alpha d\beta \right.$$
$$\left. - \int_{\Gamma^e} \bar{h} N_i l_1 d\Gamma^e + \iint_{\bar{A}^e} \bar{h} \frac{\partial N_i}{\partial \alpha} d\alpha d\beta + \iint_{\bar{A}^e} 2\dot{\bar{x}}_j \cos\alpha \, N_i d\alpha d\beta + \iint_{\bar{A}^e} 2\dot{\bar{z}}_j \cos\alpha \, N_i d\alpha d\beta \right] = 0 \qquad (3.21)$$

The equation 3.21 is written in the matrix form

$$\sum_{e=1}^{n_e} \left[\left[\bar{F}\right]^e \left\{\bar{p}\right\}^e \right] = \sum_{e=1}^{n_e} \left[\left\{\bar{Q}\right\}^e + \left\{\bar{R}_H\right\}^e + 2\dot{\bar{x}}_j \left\{\bar{R}_{xj}\right\}^e + 2\dot{\bar{z}}_j \left\{\bar{R}_{zj}\right\}^e \right]$$

Where,

$\left[\bar{F}\right]$ = Assembled Fluidity Matrix,

$\left\{\bar{p}\right\}$ = Nodal Pressure Vector,

$\left\{\bar{Q}\right\}$ = Nodal Flow Vector,

$\left\{\bar{R}_H\right\}$ = Column Vectors due to hydrodynamic terms

For e^{th} element, the components of equation 3.21 in expanded form are given as:

$$\bar{F}_{ij}^{\,e} = \iint_{\bar{A}^e} \bar{h}^3 \left[\frac{\partial N_i}{\partial \alpha} \frac{\partial N_j}{\partial \alpha} + \frac{\partial N_i}{\partial \beta} \frac{\partial N_j}{\partial \beta} \right] d\alpha d\beta \qquad (3.22a)$$

$$\bar{Q}_i^{\,e} = \int_{\Gamma^e} \left\{ \left(\bar{h}^3 \frac{\partial \bar{p}}{\partial \alpha} - \bar{h} \right) l_1 + \left(\bar{h}^3 \frac{\partial \bar{p}}{\partial \beta} \right) l_2 \right\} N_i d\bar{\Gamma}^e \qquad (3.22b)$$

$$\overline{R}^{e}_{H_i} = \iint_{\overline{A}^e} \overline{h} \frac{\partial N_i}{\partial \alpha} d\alpha d\beta \qquad (3.22c)$$

$$\overline{R}^{e}_{xji} = \iint_{\overline{A}^e} \cos\alpha \, N_i \, d\alpha d\beta \qquad (3.22d)$$

$$\overline{R}^{e}_{zji} = \iint_{\overline{A}^e} \sin\alpha \, N_i \, d\alpha d\beta \qquad (3.22e)$$

Where, l_1 and l_2 are direction cosines and i, $j = 1,2 \ldots n_l^e$.

3.2 ELASTIC DEFORMATION FIELD

For the elastic deformation analysis of the bearing shell, elasticity equations are solved. In general, the bearing shell is considered to be a three-dimensional cylindrical structure of finite length enclosed in housing. Using the linear elasticity equation, virtual work principle and finite element formulation, the system equation governing deformation in an elastic continuum is derived. Displacement at a point in the elastic solution domain is defined in terms of three components $\overline{\delta}_x, \overline{\delta}_y$ and $\overline{\delta}_z$ in the circumferential, axial and radial directions respectively. The radial component at fluid-film bush interface is needed for the computation of fluid film thickness. Generally, in practical conditions the rigidity of the journal is more as compared to that of bush and hence deformation in the journal due to fluid-film pressure has been neglected in the present study.

3.2.1 BOUNDARY CONDITIONS

The bearing shell is considered to be a three-dimensional cylindrical structure of finite length enclosed in a rigid housing. It is quite reasonable to consider the bearing shell in this manner as usually the bearing shell is made of comparatively more flexible material than the housing. Therefore, the displacement on the nodes of bush-housing interface is assumed to be zero.

$$\{\overline{\delta}\} = \begin{Bmatrix} 0 \\ 0 \\ 0 \end{Bmatrix} \qquad (3.23)$$

3.2.2 FINITE ELEMENT FORMULATION

The displacement field is discretized using three dimensional, eight-noded hexahedral isoparametric elements. By using the following non-dimensional parameters:

$$\alpha = \frac{x}{R_J}; \quad \beta = \frac{y}{R_J}; \quad \bar{r} = \frac{r}{R_J}; \quad \left[\bar{D}\right] = \frac{[D]}{E}; \quad \left\{\bar{\delta}\right\} = \frac{\{\delta\}}{c};$$

The system equation for discretized elastic continuum is defined as

$$\left[\bar{K}\right]\left\{\bar{\delta}\right\} = \bar{C}_d \left\{\bar{F}_\Gamma\right\} \tag{3.24}$$

where,

$\left[\bar{K}\right]$ = system stiffness matrix,

$\left\{\bar{\delta}\right\}$ = system nodal displacement vector,

$\left\{\bar{F}_\Gamma\right\}$ = system traction force vector,

$\bar{C}_d$ = elastic deformation coefficient.

The element stiffness matrix $\left[\bar{K}\right]$ and nodal force vector $\left\{\bar{F}_\Gamma\right\}$, for the e^{th} element are given by the following expressions:

$$\left[\bar{K}\right]^e = \int_{\Omega^e} \bar{B}^T \, \bar{D} \, \bar{B} \, \bar{r} \, d\Omega^e \tag{3.25a}$$

$$\left\{\bar{F}_\Gamma\right\}^e = \int_{\Gamma^e} N^T \, \bar{p} \, \bar{r} \, d\Gamma^e \tag{3.25b}$$

3.3 PERFORMANCE CHARACTERISTICS

The bearing performance characteristics are generally classified into two categories i.e. static and dynamic performance characteristics. The static performance characteristics include load carrying capacity, minimum film thickness, lubricant flow and attitude angle. The dynamic performance characteristics comprise of stiffness and damping coefficients, critical mass and threshold speed.

3.3.1 STATIC PERFORMANCE CHARACTERISTICS

The static performance characteristics are computed for the static condition (i.e. $\dot{\overline{X}}_J = \dot{\overline{Z}}_J = 0$) of loading. For the computation of performance characteristics it is first of all essential to establish the journal center equilibrium position for a given vertical load as described in the following subsection.

Journal centre equilibrium position

Under a given bearing, geometric parameters and for a given external vertical load, journal centre position ($\overline{X}_J, \overline{Z}_J$) is unique. For a given external load, tentative values of journal centre coordinates are fed as input. The corrections ($\Delta\overline{X}_J, \Delta\overline{Z}_J$) on the assumed journal centre coordinates ($\overline{X}_J, \overline{Z}_J$) are computed using the following algorithm. The fluid film reaction components $\overline{F}_x, \overline{F}_z$ are expressed by Taylor's series about i^{th} journal centre position. Assuming that the alteration in the journal center position are quite small and retaining terms only up to first order in the Taylor's series expansion, the corrections ($\Delta\overline{X}_J\big|_i, \Delta\overline{Z}_J\big|_j$) on the coordinates are obtained as :

$$\Delta\overline{X}_J\big|_i = -\frac{1}{D_J}\left[\left.\frac{\partial\overline{F}_z}{\partial\overline{Z}_J}\right|_i \quad -\left.\frac{\partial\overline{F}_x}{\partial\overline{Z}_J}\right|_i\right]\left\{\begin{matrix}\overline{F}_x\big|_i \\ \overline{F}_z\big|_i - \overline{W}_0\end{matrix}\right\} \tag{3.26a}$$

$$\Delta\overline{Z}_J\big|_i = -\frac{1}{D_J}\left[-\left.\frac{\partial\overline{F}_z}{\partial\overline{X}_J}\right|_i \quad \left.\frac{\partial\overline{F}_x}{\partial\overline{X}_J}\right|_i\right]\left\{\begin{matrix}\overline{F}_x\big|_i \\ \overline{F}_z\big|_i - \overline{W}_0\end{matrix}\right\} \tag{3.26b}$$

Where,

$$D_J = \left[\left.\frac{\partial\overline{F}_x}{\partial\overline{X}_J}\right|_i \left.\frac{\partial\overline{F}_z}{\partial\overline{Z}_J}\right|_i - \left.\frac{\partial\overline{F}_x}{\partial\overline{Z}_J}\right|_i \left.\frac{\partial\overline{F}_z}{\partial\overline{X}_J}\right|_i\right] \tag{3.27}$$

The new journal center position co-ordinate $\left[\overline{X}_J\big|_{i+1}, \overline{Z}_J\big|_{i+1}\right]$ are expressed as:

$$\overline{X}_J\big|_{i+1} = \overline{X}_J\big|_i + \Delta\overline{X}_J\big|_i \tag{3.28a}$$

$$\overline{Z}_J\big|_{i+1} = \overline{Z}_J\big|_i + \Delta\overline{Z}_J\big|_i \tag{3.28b}$$

The final journal equilibrium position is established using an iterative scheme.

Using the computed journal center coordinates ($\overline{X}_J$ and $\overline{Z}_J$) minimum fluid film

thickness and eccentricity ratio are computed from the expressions given below:

$$h_{\min} = \min \text{ of } \left\langle h(Eqn\,2.4c) \right\rangle_n,\ \text{n=1, 2, 3 } \ldots.\ n_l \tag{3.29}$$

Where, n_l is the number of nodes in the lubrication flow field solution domain for solving Reynold's equation.

$$\varepsilon = \sqrt{\left(\left| \overline{X}_J \right|^2 + \left| \overline{Z}_J \right|^2 \right)} \tag{3.30}$$

Load carrying capacity

Fluid film reaction components are given as

$$\overline{F}_x = -\int_{-\lambda}^{\lambda} \int_{0}^{2\pi} \overline{p} \cos\alpha \, d\alpha \, d\beta \tag{3.31a}$$

$$\overline{F}_z = -\int_{-\lambda}^{\lambda} \int_{0}^{2\pi} \overline{p} \sin\alpha \, d\alpha \, d\beta \tag{3.31b}$$

The resulting fluid film reaction is expressed as

$$\overline{F} = \left[\overline{F}^2{}_x + \overline{F}^2{}_z \right]^{1/2} \tag{3.32}$$

Attitude Angle

The attitude angle is defined as the angle between the line of action of external load, $\overline{W}_o$ and line of center. If the line of action of load (i.e. vertical load line) is taken as a reference for computing attitude angle, then for different positions of journal center, the expressions to the attitude angle is given as:

case (i)

$\overline{X}_J \geq 0.0\ ;\ \overline{Z}_J > 0.0$

$$\phi = \frac{\pi}{2} + \tan^{-1}\left[\frac{\overline{Z}_J}{\overline{X}_J} \right] \tag{3.33a}$$

case (ii)

$\overline{X}_J \leq 0.0\ ;\ \overline{Z}_J > 0.0$

$$\phi = \pi + \tan^{-1}\left| \frac{\overline{X}_J}{\overline{Z}_J} \right| \tag{3.33b}$$

case (iii)

$\overline{X}_J < 0.0\ ;\ \overline{Z}_J < 0.0$

$$\phi = \frac{3\pi}{2} + \tan^{-1}\left[\frac{\overline{Z}_J}{\overline{X}_J}\right] \tag{3.33c}$$

case (iv)

$\overline{X}_J > 0.0$; $\overline{Z}_J < 0.0$

$$\phi = \pi + \tan^{-1}\left|\frac{\overline{X}_J}{\overline{Z}_J}\right| \tag{3.33d}$$

3.3.2 DYNAMIC PERFORMANCE CHARACTERISTICS

The bearing dynamic coefficients i.e. stiffness and damping coefficient of fluid-film fall in this category. For two degree of freedom system, there exist four stiffness and four damping coefficients, which can be used to study the stability of the system. These coefficients are defined as below:

Fluid film stiffness coefficients

The fluid-film stiffness coefficients are defined as:

$$\overline{S}_{ij} = -\frac{\partial \overline{F}_i}{\partial q}(i = x, z) \tag{3.34a}$$

Where 'i' represents the direction of force and direction of displacement of journal center coordinate ($\overline{X}_J$ *or* $\overline{Z}_J$) is represented by q.

Stiffness coefficient matrix will be

$$\begin{bmatrix} \overline{S}_{xx} & \overline{S}_{xz} \\ \overline{S}_{zx} & \overline{S}_{zz} \end{bmatrix} = -\begin{bmatrix} \frac{\partial \overline{F}_x}{\partial \overline{X}_J} & \frac{\partial \overline{F}_x}{\partial \overline{Z}_J} \\ \frac{\partial \overline{F}_z}{\partial \overline{X}_J} & \frac{\partial \overline{F}_z}{\partial \overline{Z}_J} \end{bmatrix} \tag{3.34b}$$

Fluid film damping coefficients

The fluid film damping coefficients are defined as

$$\overline{C}_{ij} = -\frac{\partial \overline{F}_i}{\partial \dot{q}}(i = x, z) \tag{3.35a}$$

$\dot{q}$ represents the velocity component of journal center ($\dot{\overline{X}}_J$ *or* $\dot{\overline{Z}}_J$).

Damping coefficients matrix is given by:

$$\begin{bmatrix} \overline{C}_{xx} & \overline{C}_{xz} \\ \overline{C}_{zx} & \overline{C}_{zz} \end{bmatrix} = -\begin{bmatrix} \dfrac{\partial \overline{F}_x}{\partial \dot{\overline{X}}_J} & \dfrac{\partial \overline{F}_x}{\partial \dot{\overline{Z}}_J} \\ \dfrac{\partial \overline{F}_z}{\partial \dot{\overline{X}}_J} & \dfrac{\partial \overline{F}_z}{\partial \dot{\overline{Z}}_J} \end{bmatrix} \tag{3.35b}$$

Stability Parameters

For a very small disturbance from the equilibrium position, the hydrodynamic forces in the journal can be regarded as linear functions of the displacements and the velocity vectors. The equation of disturbed motion of the journal can be written by equating the inertia force to the stiffness and the damping forces. The linearized equation of motion of the journal in the non-dimensional form is given by:

$$\left[\overline{M}_J\right]\left\{\ddot{\overline{X}}_J\right\}+\left[\overline{C}\right]\left\{\dot{\overline{X}}_J\right\}+\left[\overline{S}\right]\left\{\overline{X}_J\right\}=0 \tag{3.36a}$$

We can write equation of motion in matrix form

$$\begin{bmatrix} \overline{M}_J & 0 \\ 0 & \overline{M}_J \end{bmatrix}\begin{Bmatrix} \ddot{\overline{X}}_J \\ \ddot{\overline{Z}}_J \end{Bmatrix}+\begin{bmatrix} \overline{C}_{xx} & \overline{C}_{xz} \\ \overline{C}_{zx} & \overline{C}_{zz} \end{bmatrix}\begin{Bmatrix} \dot{\overline{X}}_J \\ \dot{\overline{Z}}_J \end{Bmatrix}+\begin{bmatrix} \overline{S}_{xx} & \overline{S}_{xz} \\ \overline{S}_{zx} & \overline{S}_{zz} \end{bmatrix}\begin{Bmatrix} \overline{X}_J \\ \overline{Z}_J \end{Bmatrix}=\begin{Bmatrix} 0 \\ 0 \end{Bmatrix} \tag{3.36b}$$

The characteristics polynomial equation for the two-degree of freedom system is a quadric equation of the following form

$a_1s^4+a_2s^3+a_3s^2+a_4s+a_5=0$ s = complex variable (3.37)

$$a_1 = 1 \qquad > 0$$

$$a_2 = \frac{1}{\overline{M}_J}\left[\overline{C}_{xx}+\overline{C}_{zz}\right] \qquad > 0$$

$$a_3 = \frac{1}{\overline{M}_J{}^2}\left[\overline{C}_{xx}\overline{C}_{zz}+\overline{M}_J\left[\overline{S}_{xx}+\overline{S}_{zz}\right]-\overline{C}_{xz}\overline{C}_{zx}\right] \qquad > 0$$

$$a_4 = \frac{1}{\overline{M}_J{}^2}\left[\overline{S}_{xx}\overline{C}_{zz}+\overline{S}_{zz}\overline{C}_{xx}-\overline{S}_{xz}\overline{C}_{zx}-\overline{S}_{zx}\overline{C}_{xz}\right] \qquad > 0$$

$$a_5 = \frac{1}{\overline{M}_J{}^2}\left[\overline{S}_{xx}\overline{S}_{zz}-\overline{S}_{xz}\overline{S}_{zx}\right] \qquad > 0$$

Using the characteristic Equation 3.37 and Rouths' criteria, the stability margin of the journal bearing system, in terms of critical mass $\overline{M}_C$, is obtained. The system is stable when $\overline{M}_J < \overline{M}_c$. The non-dimensional critical mass $\overline{M}_c$ of the journal is expressed as

$$\overline{M}_c = \frac{\overline{G}_1}{\overline{G}_2 - \overline{G}_3} \tag{3.38}$$

$$\overline{G}_1 = \left[\overline{C}_{xx}\overline{C}_{zz} - \overline{C}_{zx}\overline{C}_{xz}\right]$$

$$\overline{G}_2 = \frac{\left[\overline{S}_{xx}\overline{S}_{zz} - \overline{S}_{zx}\overline{S}_{xz}\right]\left[\overline{C}_{xx} + \overline{C}_{zz}\right]}{\left[\overline{S}_{xx}\overline{C}_{zz} + \overline{S}_{zz}\overline{C}_{xx} - \overline{S}_{xz}\overline{C}_{zx} - \overline{S}_{zx}\overline{C}_{xz}\right]}$$

$$\overline{G}_3 = \frac{\left[\overline{S}_{xx}\overline{C}_{xx} + \overline{S}_{xz}\overline{C}_{xz} + \overline{S}_{zx}\overline{C}_{zx} + \overline{S}_{zz}\overline{C}_{zz}\right]}{\left[\overline{C}_{xx} + \overline{C}_{zz}\right]}$$

Threshold speed that is the speed of journal at the threshold of instability can be obtained using the relation given below:

$$\overline{\omega}_{th} = \left[\overline{M}_c \Big/ \overline{F}_o\right]^{1/2} \tag{3.39}$$

Where, $\overline{F}_0$ is resultant fluid film force or reaction $\left(\frac{\partial \overline{h}}{\partial \overline{t}} = 0\right)$

3.4 JOURNAL CENTER MOTION TRAJECTORIES

For a journal bearing system if journal is disturbed from its equilibrium position, experiences change in the hydrodynamic forces acting on it. This disturbs the equilibrium of the journal and makes its centre to whirl around the static equilibrium position. The dynamic response of a journal bearing system under these conditions can be obtained using either linear or non-linear equation of journal motion. These two approaches are being described in this section. The locus of the instantaneous journal centre position, as the bearing responds to a given initial disturbance, can be traced by integrating the governing equations of motion. This locus is known as the journal center motion trajectory. For simplicity, it will be referred as “linear trajectory” when it is obtained from the linear equation of motion and “nonlinear trajectory” when integrating the nonlinear equation of motion draws it.

3.4.1 LINEAR MODEL FOR MOTION TRAJECTORIES

The out of balance forces ΔF_x and ΔF_z are developed when journal is disturbed from its static equilibrium position. These forces depend on the instantaneous position and velocity of the journal centre. Mathematically, the equation of disturbed motion of the journal is written as:

$$\left[\overline{M}_J\right]\begin{Bmatrix}\ddot{\overline{X}}_J\\ \ddot{\overline{Z}}_J\end{Bmatrix}=\begin{Bmatrix}\Delta\overline{F}_x(\overline{X}_J,\overline{Z}_J,\dot{\overline{X}}_J,\dot{\overline{Z}}_J)\\ \Delta\overline{F}_z(\overline{X}_J,\overline{Z}_J,\dot{\overline{X}}_J,\dot{\overline{Z}}_J)\end{Bmatrix} \tag{3.40}$$

Where, $\left[\overline{M}_J\right]$ is a diagonal mass matrix, $\ddot{\overline{X}}_J$ and $\ddot{\overline{Z}}_J$ are the components of acceleration in **x** and **z** directions respectively.

However, within a close neighbourhood of the equilibrium position of the journal, the fluid-film forces may be assumed to be linear function of these components of displacement and velocity of the journal. Thus Equation. 3.40 may be written in terms of stiffness and damping coefficients at any time $\bar{t}$:

$$\begin{bmatrix}\overline{M}_J & 0\\ 0 & \overline{M}_J\end{bmatrix}\begin{Bmatrix}\ddot{\overline{X}}_J\\ \ddot{\overline{Z}}_J\end{Bmatrix}_{|\bar{t}}=\begin{Bmatrix}\Delta\overline{F}_x\\ \Delta\overline{F}_z\end{Bmatrix}_{|\bar{t}}=-\begin{bmatrix}\overline{S}_{xx} & \overline{S}_{xz} & \overline{C}_{xx} & \overline{C}_{xz}\\ \overline{S}_{zx} & \overline{S}_{zz} & \overline{C}_{zx} & \overline{C}_{zz}\end{bmatrix}\begin{Bmatrix}\overline{X}_J\\ \overline{Z}_J\\ \dot{\overline{X}}_J\\ \dot{\overline{Z}}_J\end{Bmatrix}_{|\bar{t}} \tag{3.41}$$

Where the subscript $\bar{t}$ refers to the instantaneous values and the stiffness and damping coefficients ($\overline{S}_{xx},\overline{S}_{xz},\overline{S}_{zx},\overline{S}_{zz},\overline{C}_{xx},\overline{C}_{xz},\overline{C}_{zx}$ and $\overline{C}_{zz}$) are evaluated at the static equilibrium position of the journal centre.

The second order Equation. 3.41 is written in the first order form by defining $\overline{X}_J=\overline{X}_1;\ \overline{Z}_J=\overline{X}_2;\ \dot{\overline{X}}_J=\overline{X}_3$ *and* $\dot{\overline{Z}}_J=\overline{X}_4$, as:

$$\begin{Bmatrix}\dot{\overline{X}}_1\\ \dot{\overline{X}}_2\\ \dot{\overline{X}}_3\\ \dot{\overline{X}}_4\end{Bmatrix}_{|\bar{t}}=\begin{Bmatrix}\overline{X}_3\\ \overline{X}_4\\ \Delta\overline{F}_x/\overline{M}_J\\ \Delta\overline{F}_z/\overline{M}_J\end{Bmatrix}_{|\bar{t}}\begin{bmatrix}0 & 0 & 1 & 0\\ 0 & 0 & 0 & 1\\ -\overline{S}_{xx}/\overline{M}_J & -\overline{S}_{xz}/\overline{M}_J & -\overline{C}_{xx}/\overline{M}_J & -\overline{C}_{xz}/\overline{M}_J\\ -\overline{S}_{zx}/\overline{M}_J & -\overline{S}_{zz}/\overline{M}_J & -\overline{C}_{zx}/\overline{M}_J & -\overline{C}_{zz}/\overline{M}_J\end{bmatrix}\begin{Bmatrix}\overline{X}_1\\ \overline{X}_2\\ \overline{X}_3\\ \overline{X}_4\end{Bmatrix}_{|\bar{t}} \tag{3.42}$$

Equation. 3.42 is numerically integrated using the fourth order Runge-Kutta method to obtain the displacement and velocity components of the journal at time $\bar{t}+\Delta\bar{t}$ in terms of the known values at time $\bar{t}$. This gives a linear trajectory.

3.4.2 NONLINEAR MODEL FOR MOTION TRAJECTORIES

When a journal is disturbed from its equilibrium position, the linearized equation of motion, Equation. 3.42 are reasonably accurate if the journal centre perturbations are very much in the close neighbourhood of the static equilibrium position. The stiffness and damping coefficients (as used in linear model) for large disturbance is no longer remain constant and their values are altered for every new position of the journal centre. Therefore, for large perturbations in the journal centre position, the linearized approach may not be accurate. In these conditions, nonlinear equations should be used. The nonlinear equation of disturbed motion of the journal may be written in terms of the instantaneous fluid film force components $\overline{F}_x$ and $\overline{F}_z$. At any time $\bar{t}$, the nonlinear equation of motion is written as:

$$\begin{bmatrix} \overline{M}_J & 0 \\ 0 & \overline{M}_J \end{bmatrix} \begin{Bmatrix} \ddot{\overline{X}}_J \\ \ddot{\overline{Z}}_J \end{Bmatrix}_{|\bar{t}} = \begin{Bmatrix} \Delta\overline{F}_x \\ \Delta\overline{F}_z \end{Bmatrix}_{|\bar{t}} = \begin{Bmatrix} \overline{F}_x - \overline{F}_{xo} \\ \overline{F}_z - \overline{F}_{zo} \end{Bmatrix}_{|\bar{t}} \tag{3.43}$$

Where, $\overline{F}_{xo}$ and $\overline{F}_{zo}$ are the fluid-film force components at the static equilibrium position. The fluid-film force components ($\overline{F}_x$ and $\overline{F}_z$) at time $\bar{t}$, are evaluated at each time step after establishing the pressure field corresponding to the position of the journal at that particular time.

The above second order differential Equation. 3.43 can be written in the first order form by following a procedure similar to the one adopted for linear equations. This gives:

$$\begin{Bmatrix} \dot{\overline{X}}_1 \\ \dot{\overline{X}}_2 \\ \dot{\overline{X}}_3 \\ \dot{\overline{X}}_4 \end{Bmatrix}_{|\bar{t}} = \begin{Bmatrix} \overline{X}_3 \\ \overline{X}_4 \\ \Delta\overline{F}_x / \overline{M}_J \\ \Delta\overline{F}_z / \overline{M}_J \end{Bmatrix}_{|\bar{t}} = \begin{Bmatrix} \overline{X}_3 \\ \overline{X}_4 \\ \overline{F}_x(\overline{X}_1, \overline{X}_2, \overline{X}_3, \overline{X}_4)/\overline{M}_J \\ \overline{F}_z(\overline{X}_1, \overline{X}_2, \overline{X}_3, \overline{X}_4)/\overline{M}_J \end{Bmatrix}_{|\bar{t}} - \begin{Bmatrix} 0 \\ 0 \\ \overline{F}_{xo}/\overline{M}_J \\ \overline{F}_{zo}/\overline{M}_J \end{Bmatrix} \tag{3.44}$$

Equation. 3.44 are integrated using the fourth order Runge-Kutta method to obtain the nonlinear trajectory when an initial disturbance in the journal position and/or velocity is given.

3.5 PROCEDURE FOR DRAWING LINEAR AND NONLINEAR TRAJECTORIES

A computer program is developed to draw the trajectories. The flow chart for drawing the trajectories is shown in the fig 3.5. Mesh data, initial perturbation, time step and related data are given as input to the computer program. Iteration counter is set equal to one initially and the program will continue to find journal centre positions till iteration counter equals maximum number of iterations. For linear trajectory ILNR=1, and for linear trajectory as described in previous section $\Delta\overline{F}_x$ and $\Delta\overline{F}_z$ is given by

$$\Delta\overline{F}_x = (\overline{C}_{xx}\dot{\overline{X}} + \overline{C}_{xz}\dot{\overline{Z}} + \overline{S}_{xx}\overline{X} + \overline{S}_{xz}\overline{Z})$$
$$\Delta\overline{F}_z = (\overline{C}_{zx}\dot{\overline{X}} + \overline{C}_{zz}\dot{\overline{Z}} + \overline{S}_{zx}\overline{X} + \overline{S}_{zz}\overline{Z})$$

For nonlinear trajectory ILNR=2, and for nonlinear trajectory instantaneous fluid film force components $\overline{F}_x$ and $\overline{F}_z$ are calculated for each journal centre position by establishing pressure field in fluid film with the help of Reynold's equation and elasticity equations. Then $\Delta\overline{F}_x$ and $\Delta\overline{F}_z$ are calculated from the following equation

$$\Delta\overline{F}_x = \overline{F}_x - \overline{F}_{xo}$$
$$\Delta\overline{F}_z = \overline{F}_z - \overline{F}_{zo}$$

Where, $\overline{F}_{xo}$ and $\overline{F}_{zo}$ are the fluid-film force components at the static equilibrium position.

Then by solving motion equations from fourth order Runga-Kutta method, next journal centre positions are obtained. Iteration counter is increased by one and the whole solution procedure repeats itself if iteration counter is less than maximum number of iteration.

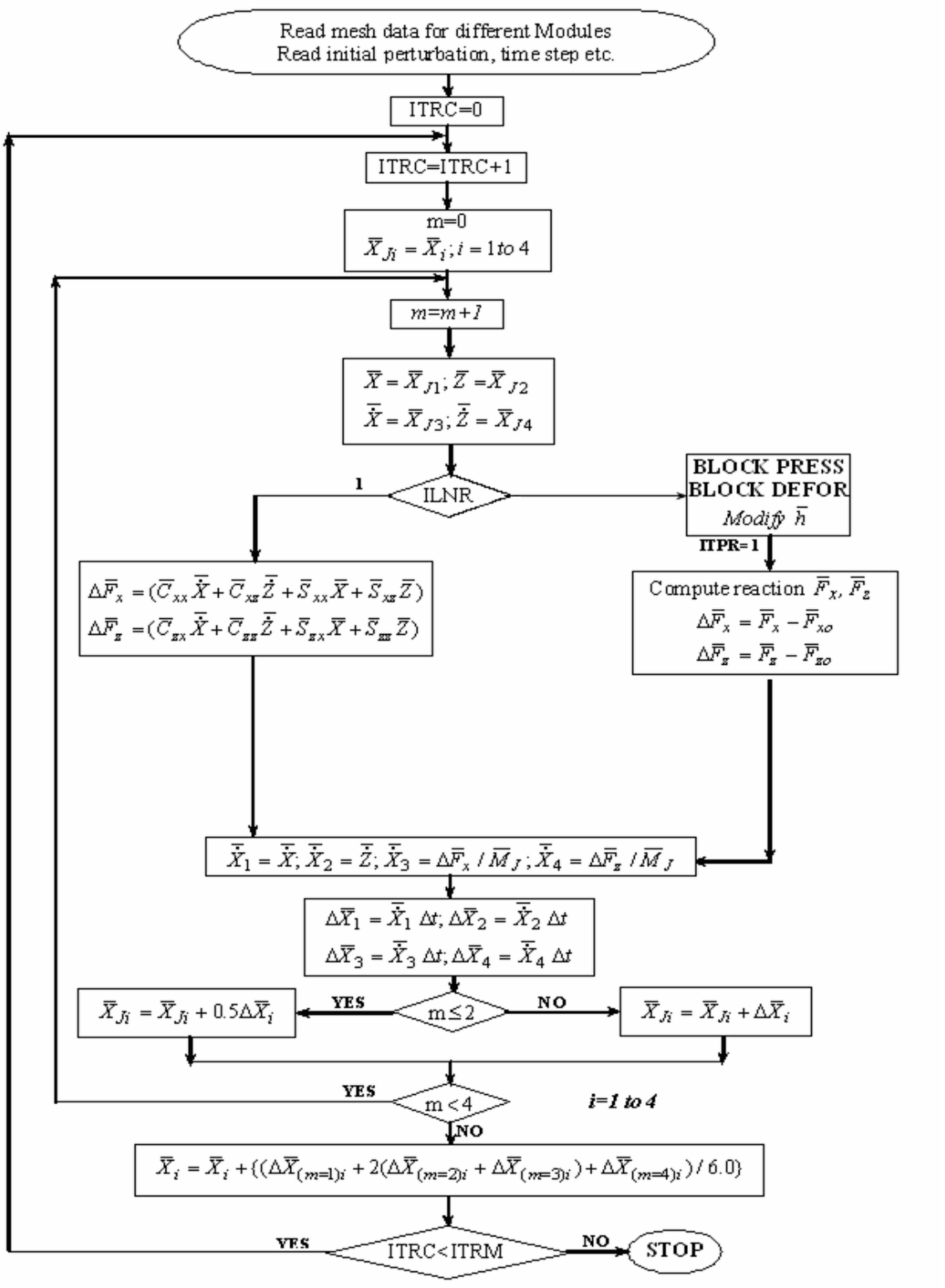

FIG.3.5

FLOW CHART FOR LINEAR AND NONLINEAR TRAJECTORIES

Chapter 4

RESULTS AND DISCUSSIONS

The linear trajectories exhibit limit cycle at $\overline{M}_J = \overline{M}_c^l$ as shown in figure 4.7 without considering elastic effects for external loads 0.5, 0.75, 1.0, 1.25, 1.5 respectively. At the same value of critical masses the nonlinear trajectories exhibits stable cycle for different loads. The journal mass is raised in increments so that nonlinear trajectory exhibits limit cycle. This journal mass is called nonlinear critical mass. The limit cycles for nonlinear trajectories are shown in figure 4.8. The values of nonlinear critical mass for different loads without considering elastic effects are tabulated in table 4.1. From table 4.1 it is observed that the journal will remain in stable zone for a higher value of critical mass obtained from linear analysis.

LOAD	LINEAR CRITCAL MASS $\overline{M}_c^l$	NONLINEAR CRITICAL MASS $\overline{M}_c^n$	APPROXIMATION IN $\overline{M}_c^l$ $\frac{\left(\overline{M}_c^n - \overline{M}_c^l\right)}{\overline{M}_c^l} \times 100$
0.50	3.215168	3.311623	3
0.75	4.813400	4.957802	3
1.00	6.406364	6.598555	3
1.25	7.830693	8.065614	3
1.50	9.472393	9.756565	3

Table 4.1

Approximation in Critical Mass without Considering Elastic Effects

In column 4 of table 4.1 approximations in linear critical mass (i.e. percentage increase in linear critical mass) are shown for various loads. The percentage increase in linear critical mass has the same value of 3% for all loads. Hence it is observed that percentage increase in linear critical mass has no effect of external load in case bearing is assumed to be rigid. The variation in linear critical mass and nonlinear critical mass with respect to external loads is shown in figure 4.1. The percentage increase in linear critical mass for different loads is shown in figure 4.4.

The figure 4.9 shows the linear and nonlinear trajectories for various loads for a flexible bearing having elastic deformation coefficient 1 for journal mass equal to linear critical mass. The figure 4.10 shows the nonlinear trajectories for journal mass equal to nonlinear critical mass. The table 4.2 shows the values of linear and linear critical mass for a flexible bearing having C_d **=1**. These values are obtained by repeating the same procedure as discussed in previous paragraphs.

LOAD	LINEAR CRITCAL MASS $\overline{M_c^l}$	NONLINEAR CRITICAL MASS $\overline{M_c^n}$	APPROXIMATION IN $\overline{M_c^l}$ $\frac{\left(\overline{M_c^n}-\overline{M_c^l}\right)}{\overline{M_c^l}}\times 100$
0.50	3.228107	3.712323	15
0.75	4.858854	5.587682	15
1.00	6.447449	7.736939	20
1.25	7.952146	9.940183	25
1.50	9.611547	12.49501	30

Table 4.2

Approximation in Critical Mass for Elastic Deformation Coefficient C_d =1

The figure 4.2 shows variation in linear critical mass and nonlinear critical mass with external load for flexible bearing having C_d =0. From figure 4.2 it is observed that variation in nonlinear critical mass is more than linear critical mass with increase in external load. The figure 4.5 shows the percentage increase in linear critical mass with external load. From figure 4.5 it is observed that variation in percentage increase in linear critical mass is almost linear.

The figure 4.11 shows the linear and nonlinear trajectories for various loads for a flexible bearing having elastic deformation coefficient 5 for journal mass equal to linear critical mass. The figure 4.12 shows the nonlinear trajectories for journal mass equal to nonlinear critical mass. The table 4.3 shows the values of linear and linear critical mass for a flexible bearing having C_d **=5**. These values are obtained by repeating the same procedure as discussed in previous paragraphs.

LOAD	LINEAR CRITCAL MASS $\overline{M_c^l}$	NONLINEAR CRITICAL MASS $\overline{M_c^n}$	APPROXIMATION IN $\overline{M_c^l}$ $\frac{\left(\overline{M_c^n}-\overline{M_c^l}\right)}{\overline{M_c^l}}\times 100$
0.75	4.982364	6.477073	30
1.00	6.617761	9.595753	45
1.25	8.209538	13.54574	65

Table 4.3

Approximation in Critical Mass for Elastic Deformation Coefficient C_d =5

The figure 4.3 shows variation in linear critical mass and nonlinear critical mass with external load for flexible bearing having C_d =5. From figure 4.6 it is observed that variation in percentage increase in linear critical mass is almost linear.

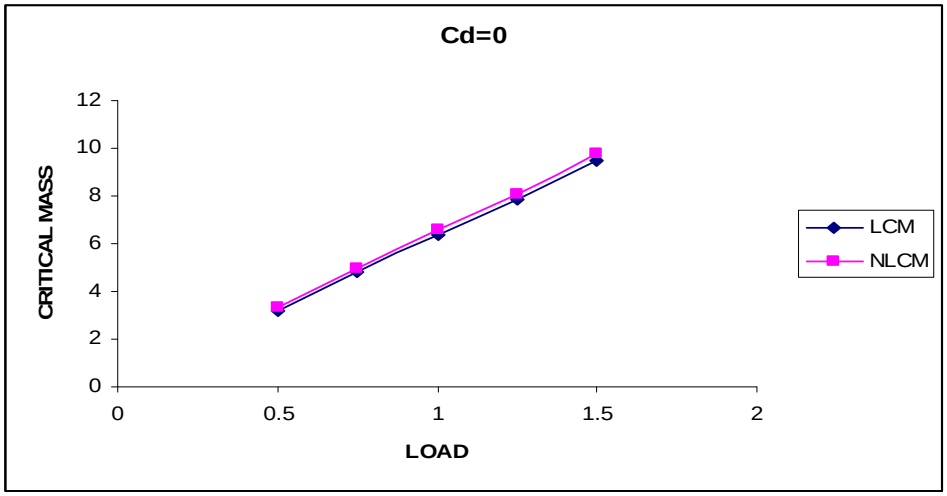

FIG. 4.1
Variation in Linear Critical Mass and Nonlinear Critical Mass with External Load

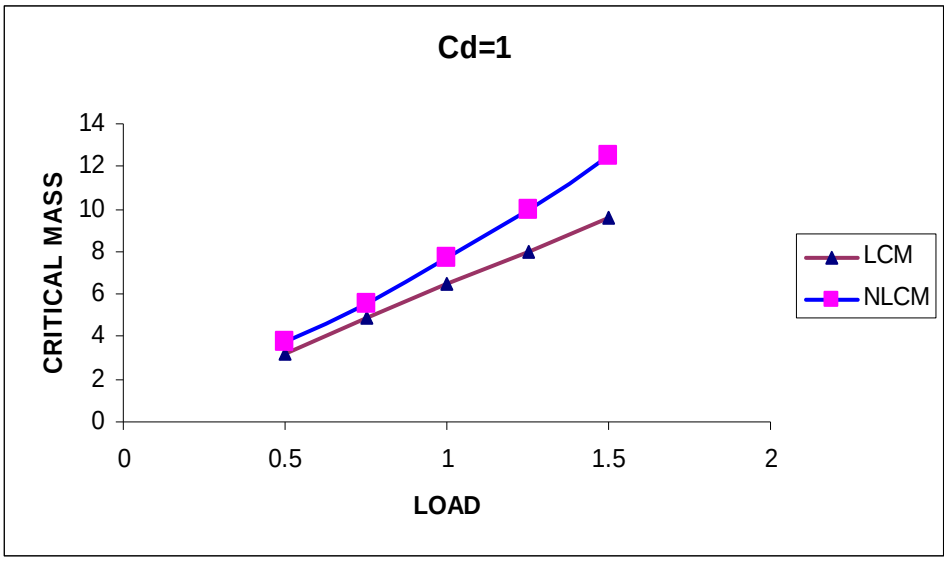

FIG. 4.2
Variation in Linear Critical Mass and Nonlinear Critical Mass with External Load for Flexible Bearing Having C_d =0.

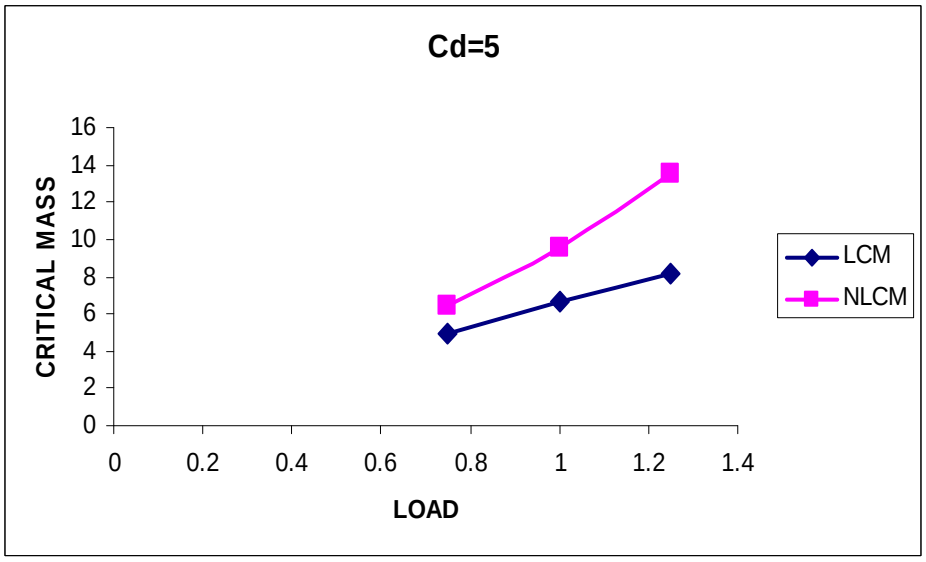

FIG. 4.3
Variation in Linear Critical Mass and Nonlinear Critical Mass with External Load for Flexible Bearing Having C_d =5.

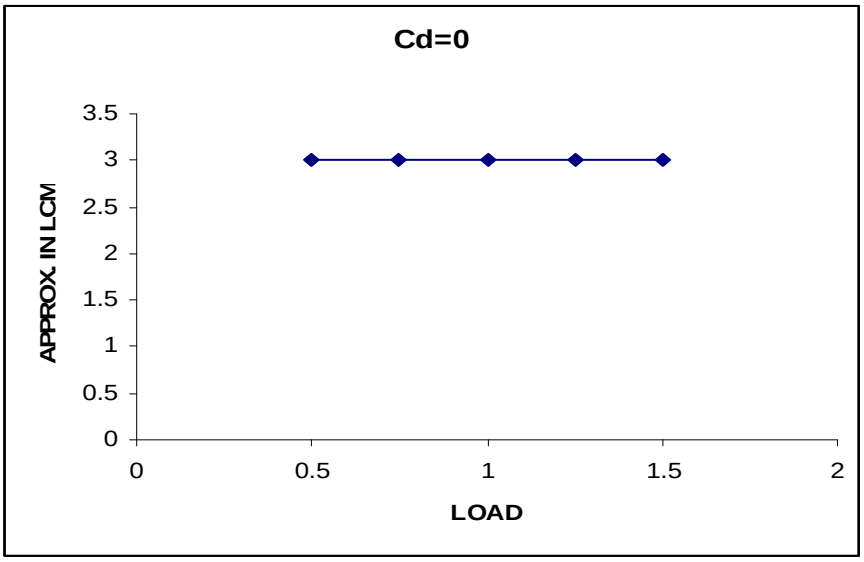

FIG. 4.4
Percentage Increase in Linear Critical Mass with Load for Rigid Bearing

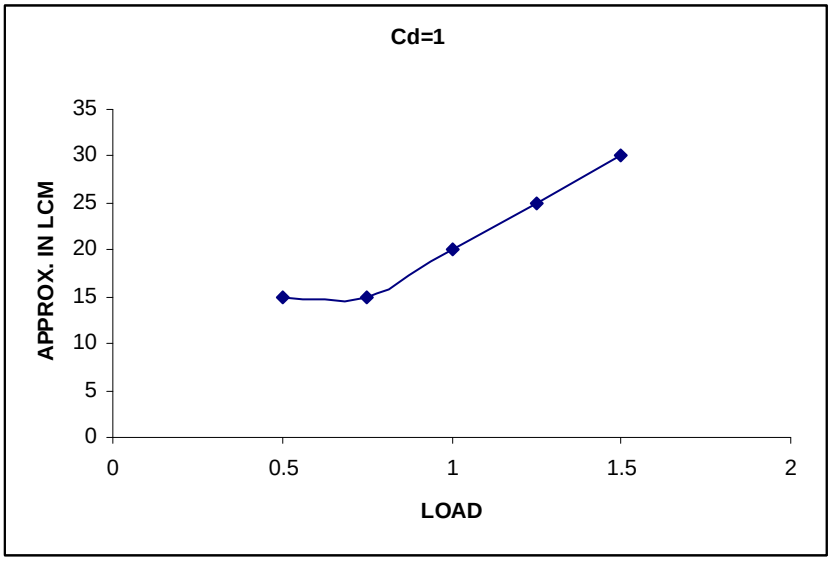

FIG. 4.5
Percentage Increase in Linear Critical Mass with Load for flexible Bearing having $C_d = 1$

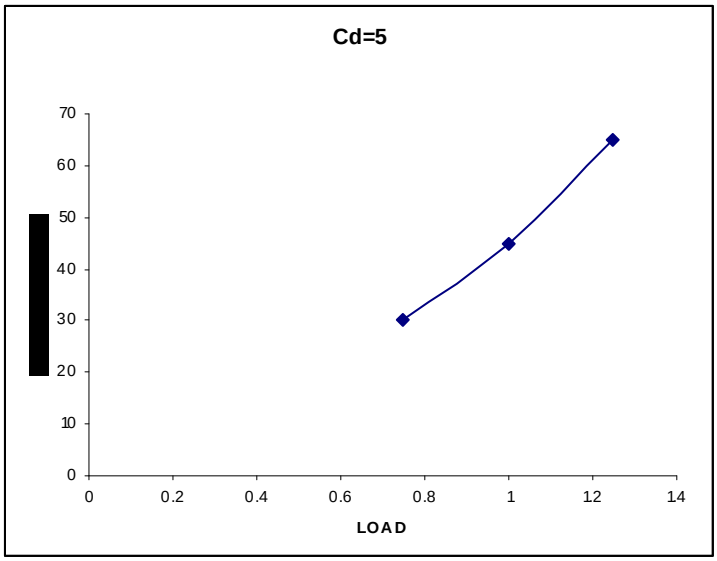

FIG. 4.6
Percentage Increase in Linear Critical Mass with Load for flexible Bearing having c_d =5

EXTERNAL LOAD	LINEAR TRAJECTORY $\overline{M}_J = \overline{M}_c^l$, c_d =0	NONLINEAR TRAJECTORY $\overline{M}_J = \overline{M}_c^l$, c_d =0
0.50	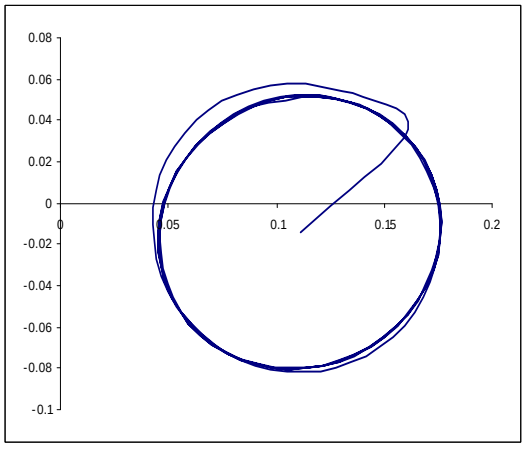	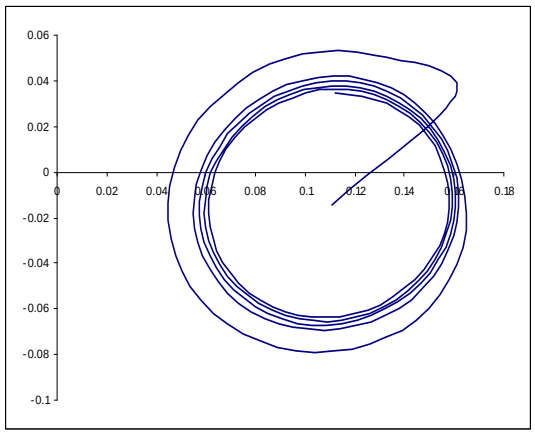

0.75	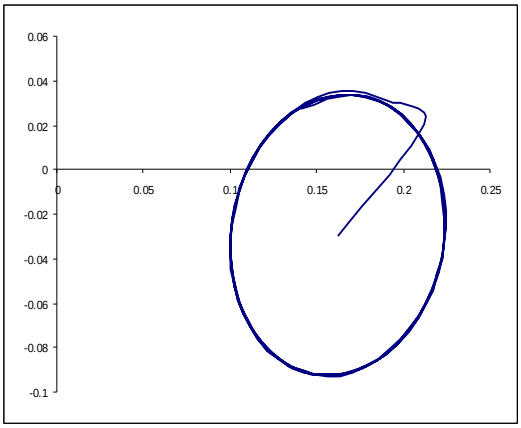 0.06 0.04 0.02 0 -0.02 -0.04 -0.06 -0.08 -0.1 0 0.05 0.1 0.15 0.2 0.25	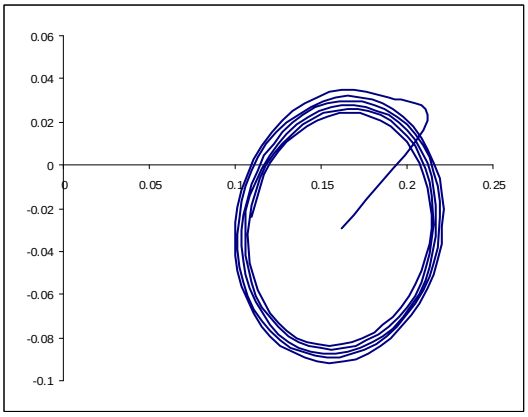 0.06 0.04 0.02 0 -0.02 -0.04 -0.06 -0.08 -0.1 0 0.05 0.1 0.15 0.2 0.25
1.00	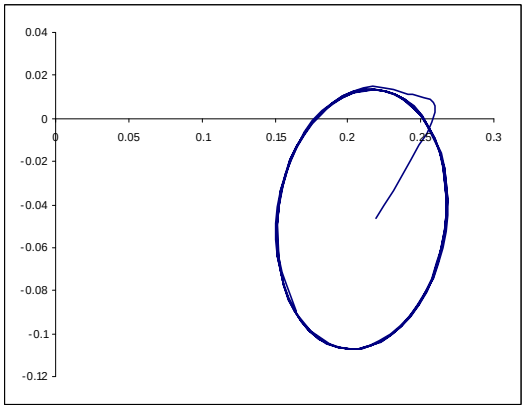 0.04 0.02 0 -0.02 -0.04 -0.06 -0.08 -0.1 -0.12 0 0.05 0.1 0.15 0.2 0.25 0.3	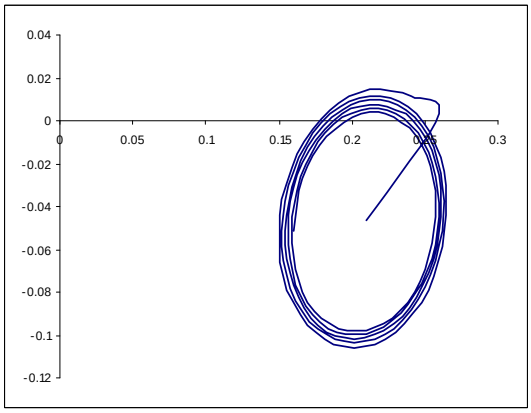 0.04 0.02 0 -0.02 -0.04 -0.06 -0.08 -0.1 -0.12 0 0.05 0.1 0.15 0.2 0.25 0.3
1.25	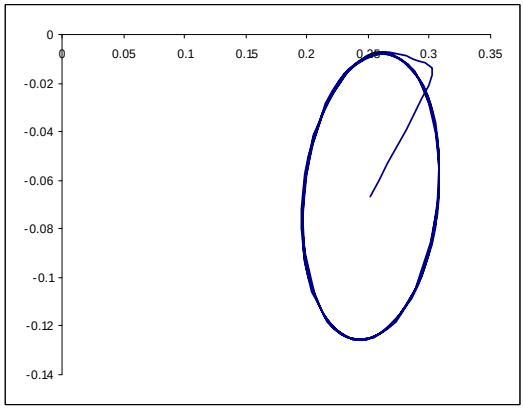 0 -0.02 -0.04 -0.06 -0.08 -0.1 -0.12 -0.14 0 0.05 0.1 0.15 0.2 0.25 0.3 0.35	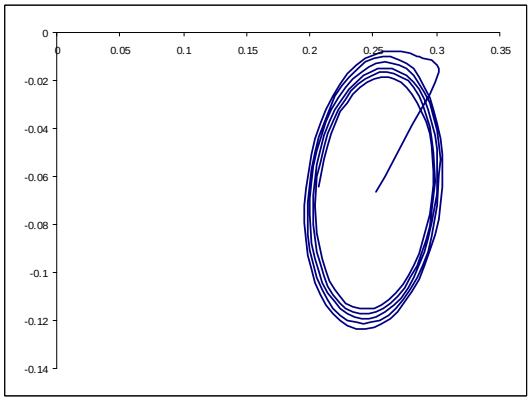 0 -0.02 -0.04 -0.06 -0.08 -0.1 -0.12 -0.14 0 0.05 0.1 0.15 0.2 0.25 0.3 0.35

1.50	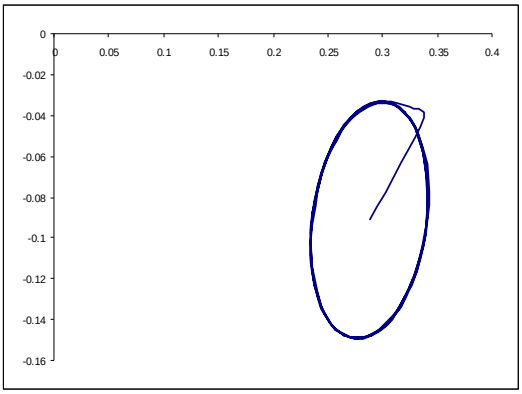	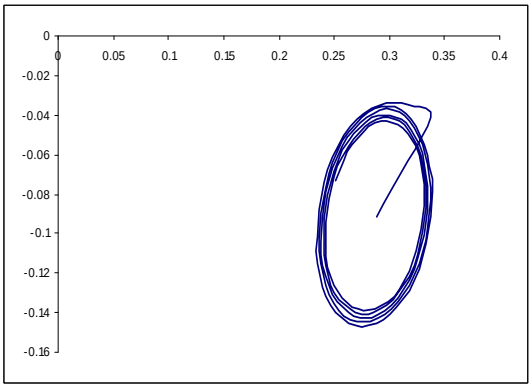

Fig. 4.7

Linear and nonlinear trajectories for various loads for rigid bearing for $\overline{M}_J = \overline{M}_c^l$.

EXTERNAL LOAD	**NONLINEAR TRAJECTORY** $\overline{M}_J > \overline{M}_c^l$, $\overline{M}_J = \overline{M}_c^n$ $c_d = 0$
0.50	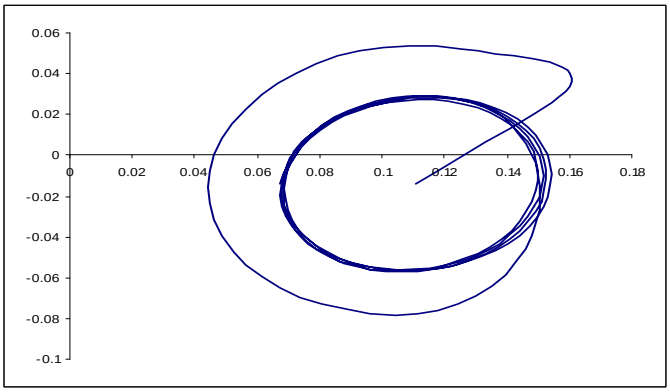
0.75	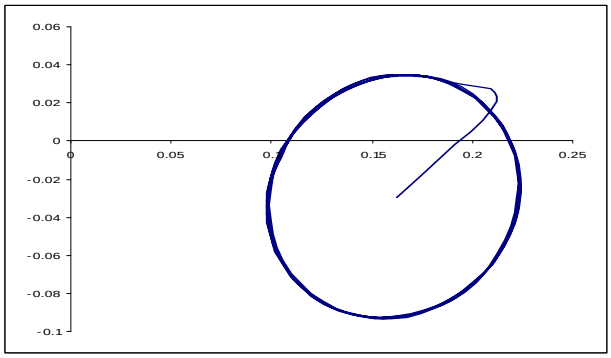

1.00	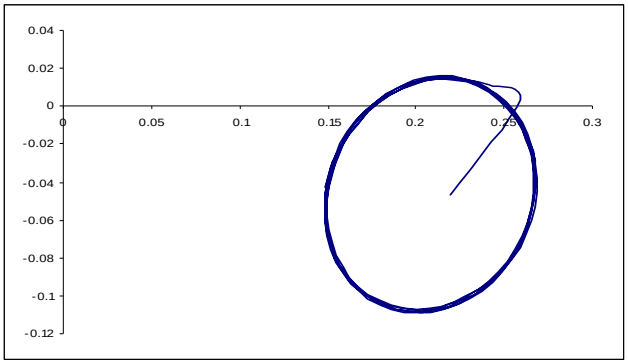
1.25	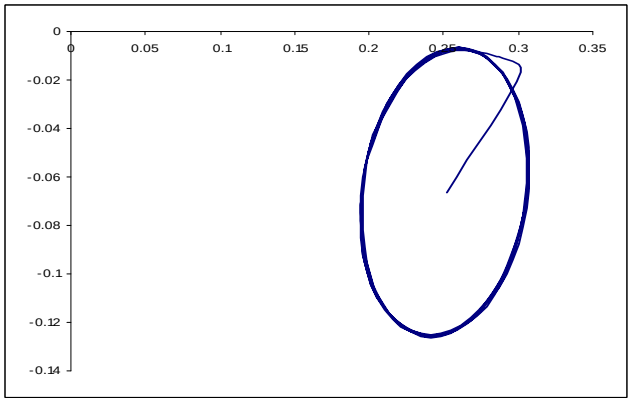
1.50	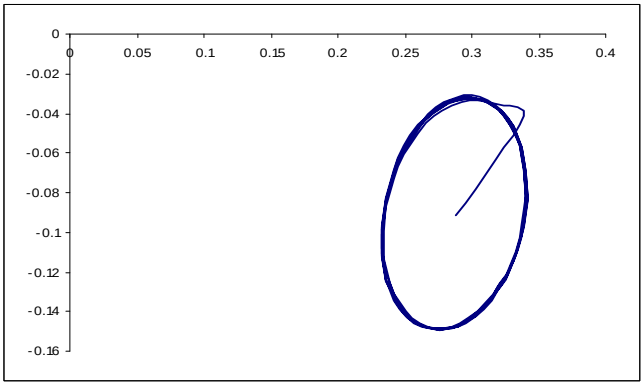

Fig. 4.8

Nonlinear Trajectories for Rigid Bearing For $\overline{M}_J = \overline{M}_c^n$

EXTERNAL LOAD	LINEAR TRAJECTORY $\overline{M_J} = \overline{M_c^l}$, $c_d = 1$	NONLINEAR TRAJECTORY $\overline{M_J} = \overline{M_c^l}$, $c_d = 1$
0.75	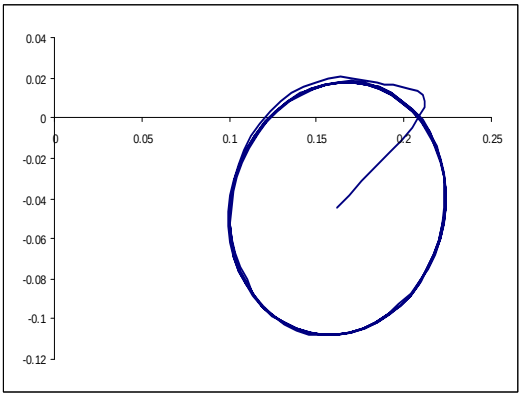	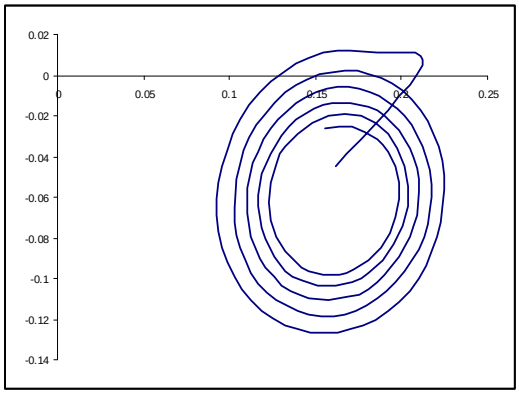
1.00	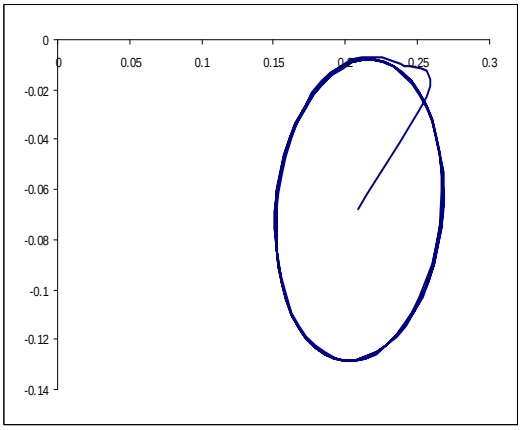	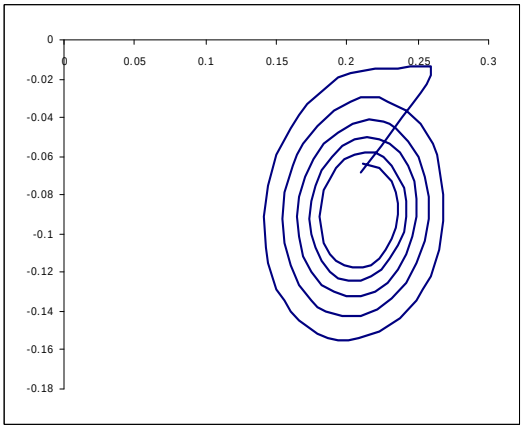
1.25	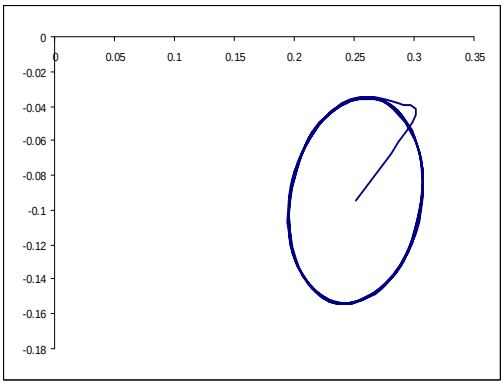	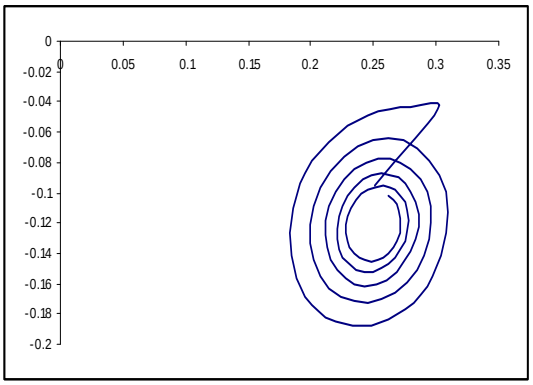

1.5	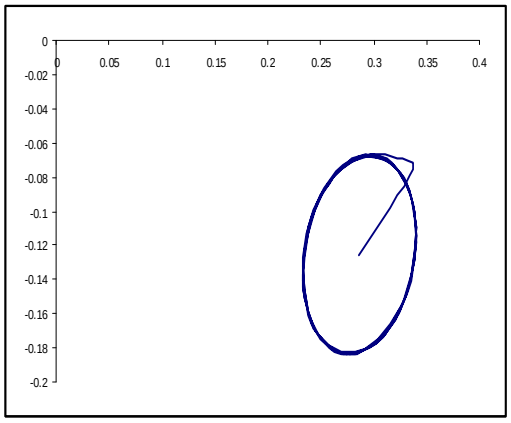	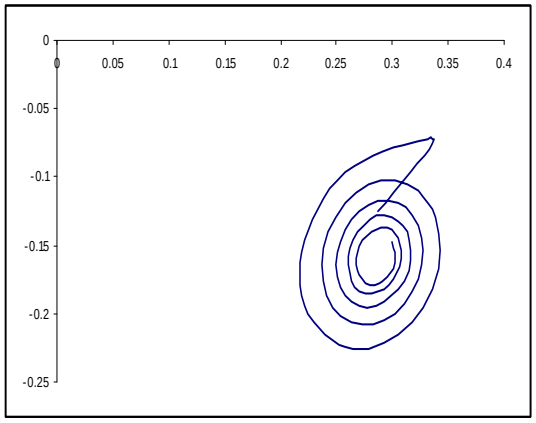

Fig. 4.9
Linear and Nonlinear Trajectories for Various Loads for Flexible Bearing Having c_d =1 For $\overline{M}_J = \overline{M}_c^l$

EXTERNAL LOAD	**NONLINEAR TRAJECTORY** $\overline{M}_J > \overline{M}_c^l$, $\overline{M}_J = \overline{M}_c^n$ c_d =1
0.75	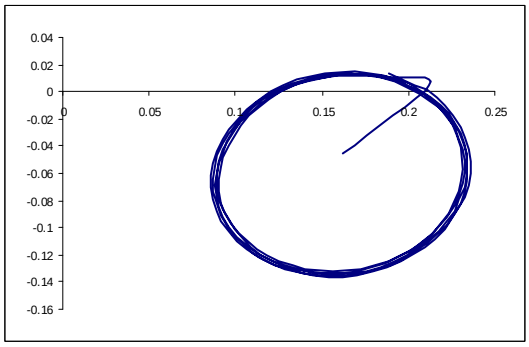

1.00	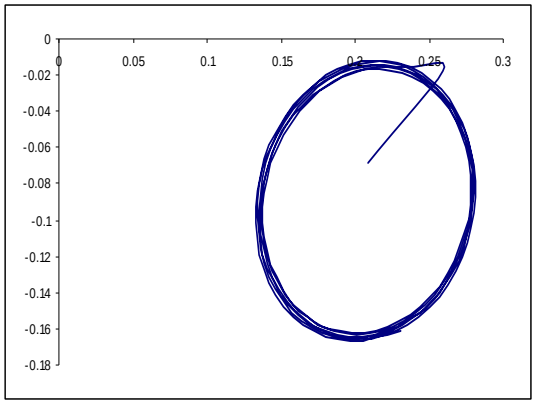
1.25	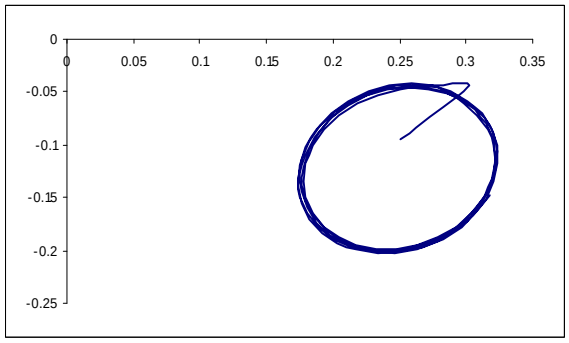
1.50	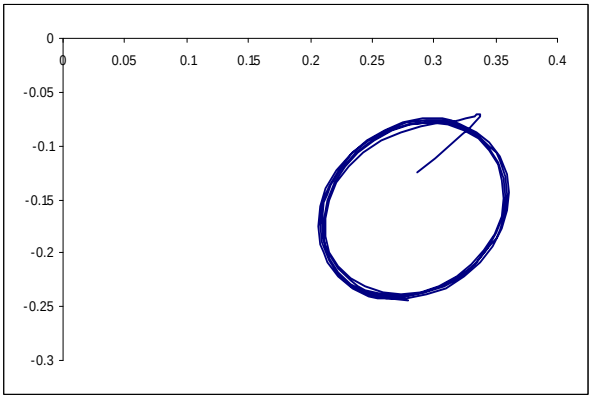

Fig. 4.10

Nonlinear Trajectories for Flexible Bearing Having C_d =1 for $\overline{M}_J = \overline{M}_c^n$

EXTERNAL LOAD	LINEAR TRAJECTORY $\overline{M}_J = \overline{M}_c^l$, c_d =5	NONLINEAR TRAJECTORY $\overline{M}_J = \overline{M}_c^l$, c_d =5
0.75	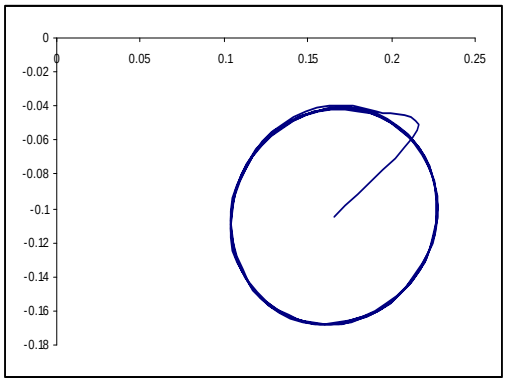	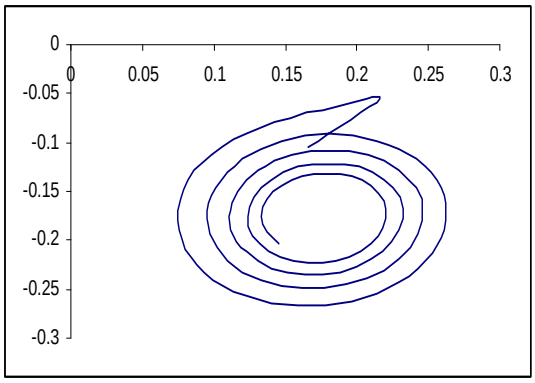
1.00	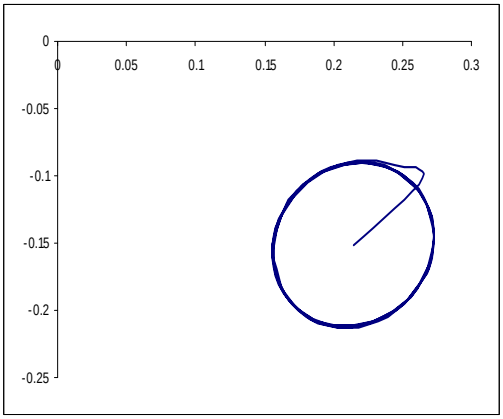	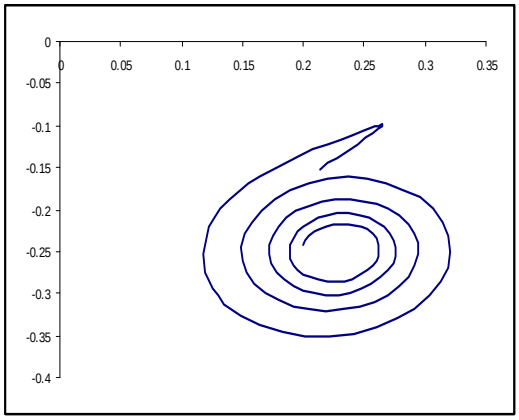
1.25	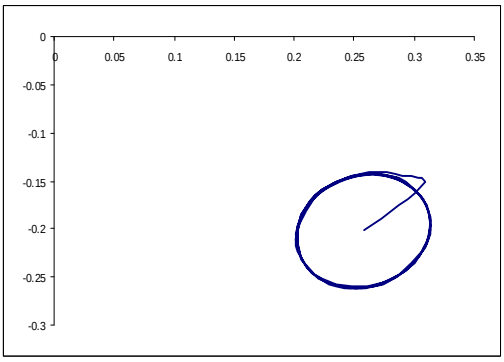	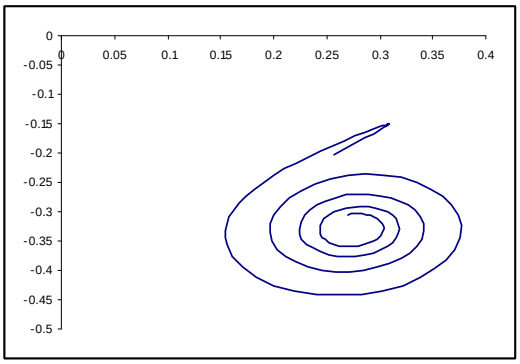

Fig. 4.11
Linear and Nonlinear Trajectories for Various Loads for Flexible Bearing Having c_d =5 for $\overline{M}_J = \overline{M}_c^l$

EXTERNAL LOAD	NONLINEAR TRAJECTORY $\overline{M_J} > \overline{M_c^l}$, $\overline{M_J} = \overline{M_c^n}$ c_d =5
0.75	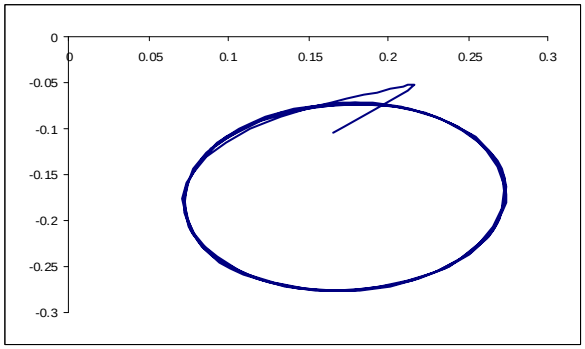
1.00	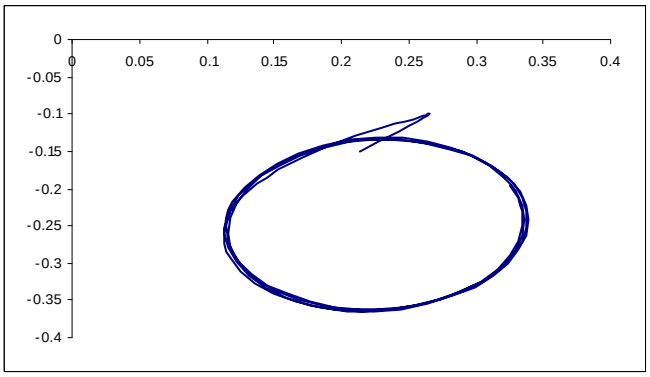
1.25	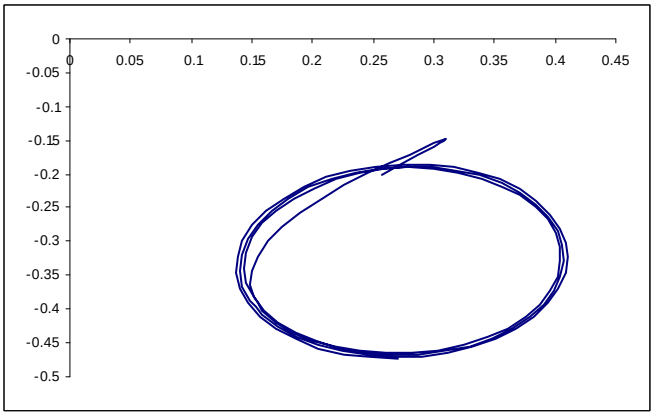

Fig. 4.12

Nonlinear Trajectories for Flexible Bearing having c_d =5 for $\overline{M_J} = \overline{M_c^n}$

Chapter 5

CONCLUSION AND SCOPE FOR FUTURE WORK

Based upon results presented in results and discussion chapter, the following conclusions have been drawn.

1. For a rigid bearing, the journal will remain in stable zone for about 3% higher value of critical mass obtained from linear formulation.
2. Increase in stability margin for rigid bearing does not change with different load values.
3. For a flexible bearing, stability margin increases with increasing external loads and this variation is almost linear.
4. A flexible bearing having higher elastic deformation coefficient has larger stability margin than bearing having lower elastic deformation coefficient.

The present work involves the study of stability margin of rigid and flexible hydrodynamic journal bearing at various loads. Further investigations may be carried out considering the following additional parameters to get more real results:

- Thermal deformation of the bearing shell.
- Misalignment of the journal in the bearing.
- Surface roughness of the bearing in transverse and longitudinal direction.

REFERENCE

1. Mokhtar, M. O. A., Howarth, R. B. and Davies, P. B., 1977, "The Behavior of Plain Hydrodynamic Journal Bearings during Starting and Stopping", Tribology Transactions, Vol.20(3), pp. 183-190.
2. Xu Shangxian, 1994, "Experimental Investigation of Hybrid Bearings", Tribology Transactions, Vol. 37(2), pp. 285-292.
3. Flack R. D., Kostrzewsky, G. J. and Taylor D. V., 1993, "A Hydrodynamic Journal Bearing Test Rig with Dynamic Measurement Capabilities", Tribology Transactions, Vol.36(4), pp. 497-512.
4. Kumar, Vijay, Sharma, S. C. and Jain, S.C., 1999, "Transient Response of Capillary Compensated Hybrid Journal Bearing System during Starting and Stopping Operation", Proc. of 2nd International conference on Industrial Tribology, Hyderabad, India, pp. 75-82.
5. Lee, A. S., Kim, B. O. and Kim, Y.C., 2006, "A Finite Element Transient Response Analysis Method of A Rotor-Bearing System to Base Shock Excitations Using the State-Space Newmark Scheme and Comparisons With Experiments", Journal of Sound and Vibration, 297, pp. 595–615.
6. Shen, G., Xiao, Z., Zhang, W. and Zheng, T.,2006 , "Nonlinear Behavior Analysis of a Rotor Supported on Fluid-Film Bearings", Journal of Vibration and Acoustics, Vol. 128, pp. 35-40.
7. Malik, M., Bhargava , S. K. and Sinhasan, R., 1989 ,"The Transient Response of a Journal in Plane Hydrodynamic Bearing during Acceleration and Deceleration Periods", Tribology Transactions, Vol.32 (1), pp. 61-69.
8. Wang, C. C., Chen C. K., 2001, "Bifurcation Analysis of Self-Acting Gas Journal Bearings", Journal of Tribology, Vol. 123, pp. 755-767.
9. Wang, J.S. and Wang, C.C., 2005, "Nonlinear Dynamic and Bifurcation Analysis of Short Aerodynamic Journal Bearings", Tribology International, 38, pp.740–748.

10. Grau, G., Iordanoff, I., Said, B. B. and Berthier, Y., 2004, “An Original Definition of the Profile of Compliant Foil Journal Gas Bearings: Static and Dynamic Analysis”, Tribology Transactions, Vol.47 (2), pp. 248-256.
11. Kakoty, S. K. and Majumdar, B. C., 2002, “Effect of Fluid Film Inertia on Stability of Flexibly Supported Oil Journal Bearings: A Non-Linear Transient Analysis”, Tribology Transactions, Vol.45 (2), pp. 253-257.
12. Malik, M., Rahmatabadi, A. D. and Jain, S. C., 1989, “An Assessment of the Stability Chart of Linearized Gas-Lubricated Plane Journal Bearing System”, Tribology Transactions, Vol.32 (1), pp. 54-60.
13. Rao, T. V. V. L. N., Biswas, S. and Athre, K., 2001, “A Methodology for Dynamic Coefficients and Nonlinear Response of Multi-Lobe Journal Bearings”, Tribology Transactions, Vol.44 (1), pp. 111-117.
14. Zhao, S., Hub, H., Menga, G. and Zhu. J., 2005, “Stability and Response Analysis of Symmetrical Single-Disk Flexible Rotor-Bearing System”, Tribology International, 38, pp. 749–756.
15. Jain, S. C., Sinhasan, R. and Pilli, S. C., 1989, “A Study on the Dynamic Response of Compliant Shell Journal Bearings”, Tribology Transactions, Vol.32 (3), pp. 297-304.
16. Kumar, Vijay, Sharma, S. C. and Jain, S.C., 1999, “On the Restrictor Design Parameter of Hybrid Journal Bearing for Optimum Rotordynamic Coefficients”, Tribology International, 39, pp.356–368.
17. Tieu, A.K., Qiu, Z. L., 1995, “Stability of Finite Journal Bearings--from Linear and Nonlinear Bearing Forces”, Tribology Transactions, Vol.38 (3), pp. 627-635.
18. Singh, D. V., Sinhasan, R. and Ghai, R. C., 1979, “Static and Dynamic Performance Characteristics of an Orifice-Compensated Hydrostatic Journal Bearing”, Tribology Transactions, Vol.22 (2), pp. 162-170.
19. Bhargava, S. K. and Malik, M., 1991, “The Transient Response of a Journal in Plane Hydrodynamic Bearing with Flexible Damped Supports During Acceleration and Deceleration Periods”, Tribology Transactions, Vol.34(1), pp. 63 – 69.

20. Wongrojn, M. M., Prabkaew, C. and Hashimoto, H., 1995, "Theoretical Prediction of Journal Centre Motion Trajectory in Two-Lobe Hydrodynamic Journal Bearings", JSME International Journal, Vol. 38(2), pp. 319- 325.
21. Malik, M. and Bhargava, S. K. ,1992, "Transient Response Investigations of Short Journal Bearing Systems with Flexible Rotors and Damped Flexible Pedestals", Tribology Transactions, Vol. 35(2), pp. 339 – 345.
22. Rao, T. V. V. L. N., Biswas, S., Hirani, H. and Athre, K., 2000, "An Analytical Approach to Evaluate Dynamic Coefficients and Nonlinear Transient Analysis of a Hydrodynamic Journal Bearing", Tribology Transactions, Vol. 43(1), pp.109 - 115.
23. Yan-jun, L. U., Lie, Y. U., Heng, L.I.U. and Yong-fang, Z., 2006, "Complex Nonlinear Behavior of a Rotor dynamical System with Non-Analytical Journal Bearing Supports", Journal of shanghai University, Vol. 10(3), pp. 247-255.
24. Meruane V. and Pascual R., 2008, "Identification of nonlinear dynamic coefficients in plain journal bearings", Tribology International.
25. Parkins, D. W., 1995, "Measurement of Oil Film Journal Bearing Damping Coefficients – an Extension of the Selected Orbit Technique", Journal of Tribology, Vol.117, pp. 696-701.
26. Choy, F. K., Braun, M. J., Hu, Y., 1991, "Nonlinear Effects in a Plain Journal Bearing: Part 1- Analytical Study", Journal of Tribology, Vol.113, pp. 555-561.
27. Prabhu, B. S., Bhat, R. B. and Sankar, T. S., 1990 "Analytical Methods for Rotors Supported on Hydrodynamic Journal Bearings", Tribology Transactions, Vol.33(1), pp. 60 – 66.
28. Turaga, Ram, Sekhar, A. S. and Majumdar, B. C., 2000, "Non-Linear Transient Stability Analysis of a Rigid Rotor Supported on Hydrodynamic Journal Bearings with Rough Surfaces", Tribology Transactions, Vol. 43(3), pp. 447 – 452.
29. Choy, F. K., Braun, M. J., Hu, Y., 1992, "Nonlinear Transient and Frequency Response Analysis of a Hydrodynamic Journal Bearing", Journal of Tribology, Vol. 114, pp. 448-454.
30. Brancati, R., Rocca, E., Russo, M., 1995, "Journal Orbits and their Stability for Rigid Unbalanced Rotors", Journal of Tribology, Vol. 117, pp. 709-716.

31. Kumar, Vijay, Sharma, S. C. and Jain ,S. C., 2004, “Stability Margin of Hybrid Journal bearings influence of thermal and elastic effects”, Journal of Tribology, Vol. 126, pp. 630-634.